Periodico di Mineralogia (2011), 80, 3 (Spec. Issue), 489-515 DOI: 10.2451/2011PM0032

PERIODICO di MINERALOGIA
established in 1930

An International Journal of
MINERALOGY, CRYSTALLOGRAPHY, GEOCHEMISTRY, ORE DEPOSITS, PETROLOGY, VOLCANOLOGY
and applied topics on *Environment*, *Archeometry* and *Cultural Heritage*

Late-Hercynian post-collisional dyke magmatism in central Calabria (Serre Massif, southern Italy)

Vanessa Romano[1,*], Rosolino Cirrincione[1], Patrizia Fiannacca[1], Michele Lustrino[2, 3] and Annunziata Tranchina[1]

[1] Dipartimento di Scienze Geologiche, Università degli Studi di Catania, C.so Italia 57, 95129 Catania, Italy
[2] Dipartimento di Scienze della Terra, Università degli Studi di Roma La Sapienza, P.le A. Moro 5, 00185 Roma, Italy
[3] Istituto di Geologia Ambientale e Geoingegneria (CNR - IGAG) Roma, Italy
*Corresponding author: *vanessa.romano@unict.it*

Abstract

Widespread late- to post-collisional magmatism occurred in the Calabria-Peloritani Orogen (southern Italy) during the final stages of the Hercynian Orogeny. In the Serre Massif (central Calabria), medium- to high-K calcalkaline andesitic to dacitic-rhyodacitic dykes show typical geochemical features of subduction-related magmas (LILE and LREE enrichment, HFSE depletion, peaks at Rb, Pb and Th). The origin of late- to post-Hercynian calcalkaline rocks is usually interpreted in an extensional post-collisional framework, involving thinning of the continental lithosphere and progressive passive upwelling of the asthenospheric mantle. In such a context, pure mantle, crustal and hybrid melt production likely can occur. The andesitic dykes were produced by partial melting of an enriched mantle source metasomatized by crustal fluids/melts during former subduction and then suffered minor, if any, assimilation of lower crustal metapelites. Most dacite-rhyodacites were likely derived by hybridization in various proportions of crustal and mantle melts, whereas pure crustal metasedimentary sources, and more or less efficient restite unmixing processes, were involved in the generation of the most silica-rich rhyodacites.

Key words: post-collisional dyke magmatism; andesite; dacite-rhyodacite; Serre Massif; Calabria-Peloritani Orogen.

Introduction

During the late Paleozoic to Early Triassic, a felsic-intermediate and minor mafic magmatism extensively affected large areas of the European Hercynian Belt. Examples are reported from the Pyrenean Chain (e.g., Innocenti et al., 1994; Lago et al., 2004), the French Massif Central (e.g., Ledru et al., 2001; Perini et al., 2004), the Bohemian Massif (e.g., Janousek et al., 2000; Ulrych et al., 2006), the Spanish Central System (e.g., Perini et al., 2004; Orejana et al., 2008), the

Sardinian-Corsica Domain (e.g., Traversa et al., 2003; Bonin, 2004) as well as from the Calabria-Peloritani Orogen (Rottura et al., 1990; 1993; Cirrincione et al., 1995; Fiannacca et al., 2008).

Two chronologically, geochemically and mineralogically different magmatic episodes are recognized (Cortesogno et al., 1998; 2004a; Bonin et al., 1998; Bonin, 2004; Rottura et al., 1998; Traversa et al., 2003). The first igneous activity - developed mostly during the Late Carboniferous-Early Permian - produced sub-alkaline low- to high-K calcalkaline magmas (Cortesogno et al., 1998; 2004a; Cassinis et al., 2008), whereas the latter - mostly Late Permian-Early Triassic - produced transitional to Na-alkaline magmas (Bonin, 1989; Bonin et al., 1998; Cortesogno et al., 1998; 2004b).

Petrogenetic models and geodynamic interpretations proposed for these magmatic events are still matter of debate. In particular, one of the main object of diatribe concerns the geodynamic significance of the magmas belonging to the first cycle, typically showing convergent plate margin geochemical features (Lorenz and Nicholls, 1984; Finger and Steyrer, 1990; Dal Piaz and Martin, 1998). Partially in contrast with this geological reconstructions suggest a post-collisional context and a transtensional regime, developed within an over-thickened continental crust suffering a gravity collapse of the main chain, associated with the formation of intermontane troughs (Arthaud and Matte, 1977; Ziegler, 1993; Cortesogno et al., 1998; 2004a; Lustrino, 2000). The occurrence of igneous activity with subduction-related geochemical characteristics in post-collisional settings (e.g., after the end of the oceanic lithosphere subduction) is an anomalous feature, recorded also in other younger orogens, like the Alpine Chain (e.g., Rosenberg, 2004; Lustrino et al., 2011 and references therein).

The Late Permian-Early Triassic phase, characterized by basic-intermediate Na-alkaline magmas up to evolved compositions (e.g., hawaiitic to A-type rhyolitic dykes in Sardinia and Corsica; Atzori and Traversa, 1986; Bonin, 1989; Bonin et al., 1998; Traversa et al., 2003), is instead mostly interpreted as a typical intra-plate event preluding to continental break-up and subsequent formation of the Neotethys (e.g., Stampfli et al., 2002).

The present paper focuses the attention on the products of the first phase of activity, cropping out diffusely in the Serre Massif (central Calabria). They consist of calcalkaline intermediate-to-felsic dykes that intrude the metamorphic basement as well as late Hercynian granitoids. The aim of this work is to study petrographic, mineral chemical and geochemical features of these dykes in order to develop a petrogenetic model to explain their origin and to give a contribution on the Late Palaeozoic geodynamic evolution of the southern European Hercynian Belt.

Geological background and field features

The studied dykes crop out in four different areas of the central sector of the Calabria-Peloritani Orogen (hereafter CPO; Figure 1). The CPO is an arcuate orogenic belt bounded by two main tectonic lineaments: the Sangineto line to the North, and the Taormina line, to the South (Tortorici, 1982; Figure 1). The nappe system of the CPO includes several tectonic slices of basement rocks and Mesozoic-Cenozoic sedimentary sequences.

Three are the main hypotheses proposed to explain the origin and geodynamic significance of the CPO:

the CPO would represent a fragment of the Alpine orogenic belt, belonging to the western margin of Adria, emplaced north-westward onto Tethyan ophiolites (Late Cretaceous-Paleogene) (Haccard et al., 1972; Alvarez, 1976; Amodio-Morelli et al., 1976) and later overridden on the Apennine domains (Late Oligocene-Early Miocene);

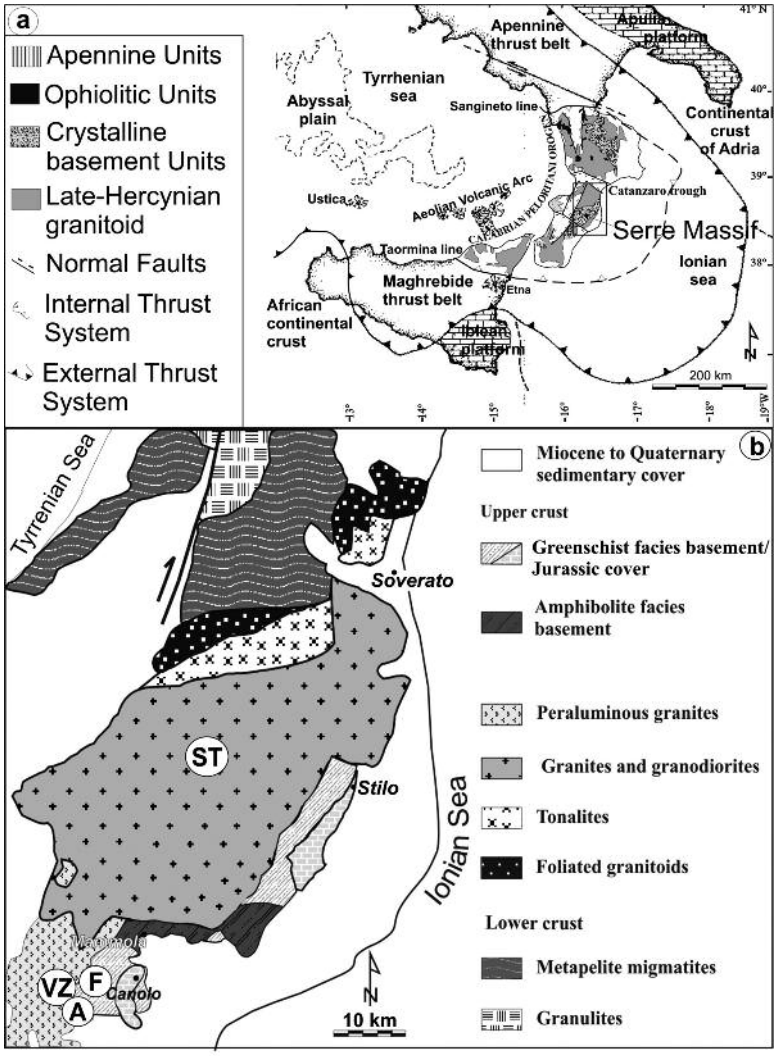

Figure 1. a) Geological-structural sketch-map of the south-western Mediterranean area (from Ortolano et al., 2005, modified). b) Geological sketch map of the Serre Massif (Southern Calabria-Peloritani Orogen) (Graessner et al., 2000, modified) with location of studied dykes. ST: San Todaro; A: Antonimina; VZ: Villaggio Zomaro; F: Foletti Valley.

the CPO would represent a fragment of the southern European continental paleo-margin, thrust and folded south-eastward onto the Adria margin, starting from middle Miocene, contemporaneously with the opening of the Tyrrhenian Sea (Ogniben, 1969; Bouillin et al., 1986; Knott, 1987; Dewey et al., 1989);

the CPO would represent a micro-continent located between two continental margins, European and African, separated from them by

two Tethyan branches and later involved in Europe-Adria collision (Doglioni, 1992; Guerrera et al., 1993; Critelli and Le Pera, 1998; Gueguen et al., 1998; Lustrino et al., 2009; Tortorici et al., 2009; Carminati et al., 2010).

The CPO is classically subdivided into a northern and southern sector, separated along the Catanzaro trough (Tortorici, 1982). The main differences between the two sectors are the lack of ophiolitic units in the southern segment and the presence of an originally Europe-verging chain in the northern-western sector in contrast with exclusively Africa-verging thrusts in the southern one.

The studied dykes crop out in the central part and in the south-western termination of the Serre Massif belonging to the southern sector of the CPO. According to Schenk (1980; 1984; 1990), the Serre Massif represents one of the few places in the world where a nearly complete section of continental crust, with an overall thickness of about 30 km, is exposed. The crustal section is made up of (from the bottom to the top):

a) lower crustal metagabbros, felsic and mafic granulites, and metapelitic migmatites (Schenk, 1980; 1984; 1990; Acquafredda et al., 2006);

b) large bodies of late Hercynian metaluminous to weakly peraluminous granodiorites and tonalites, and minor strongly peraluminous granodiorites and granites, forming the Serre batholith, intruded in between the lower and upper crustal metamorphic rocks (Rottura et al., 1990; Caggianelli et al., 2007 and references therein);

c) greenschist to amphibolite facies metasedimentary and minor metavolcanic sequences, forming the uppermost crustal levels (Colonna et al., 1973; Atzori et al., 1977; Acquafredda et al., 1987; Angì et al., 2010).

Two magmatic suites have been recognized in the Serre batholith: a main metaluminous-to-weakly-peraluminous calcalkaline group, representing about the 70% of the exposed granitoids, and a less extensive suite of strongly peraluminous rocks (Rottura et al., 1990; 1993; Caggianelli et al., 2007 and references therein). The first group of rocks show a broad compositional range (~ 48-70 wt. % SiO_2), with tonalites and granodiorites being the dominant rock types. The strongly peraluminous plutonic rocks lack basic to intermediate lithologies (~ 67-76 wt. % SiO_2) and contain the typical paragenesis of two micas ± Al-silicates. The metaluminous-to-weakly-peraluminous granitoids have been interpreted as I-type rocks resulting from the interaction of mantle-derived magmas with lower-crustal melts (Rottura et al., 1990), whereas the strongly peraluminous granitoids have been interpreted either as typical S-type granites, with sedimentary source rocks (D'Amico et al., 1982; Rottura et al., 1990), or as magmas with mixed mantle-crust origin (Rottura et al., 1991; 1993). According to the previous authors, all the plutonic rocks were emplaced in an extensional regime, during late- to post-collisional phases in the frame of the Hercynian Orogeny. Early geochronological data for the timing of Hercynian magmatism in southern CPO, gave ages spanning the Paleozoic-Mesozoic boundary (from ~ 298 ± 5 to ~ 270 ± 5 Ma; Rb-Sr whole-rock and mineral ages, zircon U-Pb ages; Borsi and Dubois, 1968; Borsi et al., 1976; Schenk, 1980; Del Moro et al., 1982). More recently, strongly peraluminous granites (Cittanova granite) intruding the Serre batholith in its south-western sector, have been dated by ID-TIMS monazite at 303 ± 0.6 Ma (Graessner et al., 2000) falling in the range of ~ 304-300 Ma obtained for the strongly peraluminous magmatism in the whole CPO (ID-TIMS monazite and xenotime ages and SHRIMP zircon ages; Graessner et al., 2000; Fiannacca et al., 2008).

Different populations of dykes intrude the plutonic rocks of the Serre batholith as well as the surrounding basement rocks. These dykes have been classified as porphyritic rhyolites, aplites, microgranites and dacites, and include also minor mafic types (Colonna et al., 1973; Borsi et al., 1976; Atzori et al., 1981). Very little

is still known about their geochemistry, age, as well as their origin and geodynamic scenario of emplacement. This work aims to investigate four groups of intermediate to felsic dykes. Cropping out in central-southern Serre Massif, in the San Todaro, Foletti Valley, Antonimina and Villaggio Zomaro areas (labelled as ST, F, A and VZ in Figure 1, respectively). The ST dykes are all porphyritic and intrude amphibole-biotite-bearing tonalites and biotite granodiorites. They are dark brown, 1 to 10 m-wide dykes, with tabular or lenticular shape. The grey-green F dykes intrude the phyllite basement with discordant relationships and an average width of 6 m. The light grey A dykes intrude two-mica peraluminous granites and range in width from 0.5 to 3 m. Lastly, the grey-green VZ dykes cut the same peraluminous granites cut by the A dykes with a width ranging from 0.5 to 6 m.

Analytical methods

Whole-rock compositions of 43 samples were determined by X-ray fluorescence (XRF) on powder pellets, corrected for matrix effects (Franzini et al., 1975), at the Dipartimento di Scienze Geologiche, University of Catania. XRF analyses were carried out on a Philips PW 2404 spectrometer, equipped with a Rh anticathode, on pressed powder pellets. Volatile content was measured as loss on ignition (L.O.I.) by standard gravimetric method. Trace element concentrations were obtained by ICP-MS at SGS Mineral Services (Toronto, Canada). 56 elements are detected by sodium peroxide fusion that involves the complete dissolution of the sample in a molten flux. Mineral compositions were obtained using a WDS/EDS-equipped CAMECA SX50 electron microprobe at Istituto di Geologia Ambientale e Geoingegnereia (IGAG)-CNR, Rome, with silicates and oxides as standards, and by SEM-EDS analyses at the Dipartimento di Scienze Geologiche, University of Catania using a Tescan Vega LMU scanning electron microscope equipped with an EDAX Neptune XM4-60 micro-analyzer characterized by an ultra-thin Be window. Analyses were performed at 20 kV accelerating voltage and 0.2 nA beam current. Precision of collected data is on the order of 5%.

Petrography and mineral chemistry

All the samples show a porphyritic texture, with a relatively high Porphyritic Index (P.I.) in F samples. Magmatic assemblages are commonly replaced by secondary mineral associations formed during hydrothermal alteration.

Group A dykes have a P.I. of ~ 10-15%, with abundant clinopyroxene, and much rarer amphibole and plagioclase phenocrysts. The same phases are present also in the microcrystalline groundmass, together with rare K-feldspar microlites. Colorless clinopyroxene phenocrysts are often fractured and disarticulated, and show corroded cores commonly replaced by chlorite. Brown to pale green amphibole phenocrysts and microcrysts are typically replaced by actinolite. Plagioclase phenocrysts and microcrysts are extensively sericitized. Accessory phases are represented by ilmenite, titanite and apatite. Zircons are very rare and tiny. Among the secondary phases, chlorite, sericite and epidote are the most abundant.

Group F dykes show porphyritic texture (P.I. ~ 20-25%) with clinopyroxene and amphibole phenocrysts set in a fine-grained groundmass made up of plagioclase, K-feldspar, quartz and amphibole. Clinopyroxene phenocrysts are commonly extensively transformed into chlorite and actinolite aggregates. Hornblende is characterized by high relief, marked cleavage and pleochroism ranging from pale yellow to green. Actinolite replacements are often present at the rim of hornblende phenocrysts, more rarely as total pseudomorphosis. Plagioclase is nearly absent among phenocrysts and is confined to groundmass as extensively sericitized and saussuritized laths. Micrographic intergrowths of quartz and K-

feldspar are also present in the groundmass. Accessory phases consist of ilmenite, apatite, titanite and few and tiny zircon grains. Secondary minerals include chlorite, epidote, sericite and calcite.

Group VZ dykes show porphyritic phaneritic texture (P.I. ~ 10-15%) with K-feldspar phenocrysts in a medium-grained groundmass made up of subhedral to anhedral and radiating quartz, K-feldspar and white mica. K-feldspar phenocrysts have suffered extensive alteration processes that produced opaque and clay minerals. Quartz rims around K-feldspar phenocrysts suggest reaction processes between phenocrysts and melt. Quartz *ocelli*, ~ 1.5-2.0 mm in size, commonly occur as large rounded quartz grains with a K-feldspar and quartz coronitic texture. Local embayment suggest corrosion during melt solidification. Accessory phases are rutile, apatite and zircon. Secondary minerals consist of clay minerals, epidote and white mica.

Group ST dykes can be subdivided in two sub-groups in function of textural and mineralogical features: group I, characterized by a porphyritic texture, with a fine-grained matrix and white mica-poor secondary assemblage; group II, characterized by a porphyritic to equigranular texture with a fine to medium-grained matrix, by the presence of abundant interstitial and radial white mica and by micrographic and radiating intergrowths of quartz and K-feldspar. The P.I. is very low (< 7%), with extensively altered K-feldspar and plagioclase phenocrysts. Matrix phases consist of plagioclase, K-feldspar, quartz, chloritized biotite and opaque minerals. Among the phenocrysts, former mafic minerals, possibly amphibole and biotite, have been completely replaced by chlorite. Zircon, rutile and apatite occur as accessory phases.

Pyroxene

In group A samples, clinopyroxene is augite (Wo_{22-48}-En_{37-64}-Fs_{5-36}; Figure 2; Table 1) apart from few crystals that fall in the diopside field (Morimoto, 1988). They all have high MgO (11.0-19.9 wt.%) and CaO contents (10.4-21.3 wt.%); FeO ranges between 2.9 and 13.6 wt.%, with very low TiO_2 and Na_2O contents (0.23-1.05 wt.%; 0.00–1.66 wt.%, respectively). Mg# value [$Mg/(Mg+Fe^{2+})$] ranges between 0.69 and 0.88. A slight decrease in Mg#, MgO and CaO and increase in Al_2O_3, FeO and TiO_2 contents, is recorded from core to rim, defining a normal compositional zoning.

Various attempts to determine the composition of the pyroxenes of F dykes did not provide reliable data, probably due to difficulty of obtaining clean analyses in the tiny portions of the crystals apparently spared by chlorite/actinolite replacement.

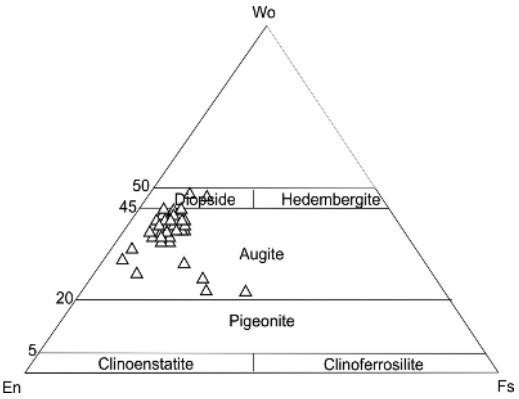

Figure 2. Clinopyroxene microprobe compositions from A dykes in the Ca-Mg-Fe^* ($Fe^* = Fe^{2+}+Fe^{3+}+Mn$) classification diagram (Morimoto, 1988).

Amphibole

Amphiboles found in Serre dykes are all calcic and are represented by tschermakite and Mg-hornblende in group A samples (according to Leake et al., 1997; Figure 3 and Table 1); the latter composition also occurs in group F samples. Mg# value of the Mg-hornblende range from 0.62 to 0.77, and from 0.73 to 0.98 in A and F dykes, respectively. TiO_2 contents ranges

Table 1. Representative major element composition of clinopyroxene and amphibole from Serre dykes.

	Clinopyroxene								Amphibole				Amphibole			
Sample	A1a								A1a				F8			
Analyses	1	2	3	4	5	6	7	8	1	2	3	4	1	2	3	4
SiO_2	50.39	52.81	53.43	54.50	53.24	54.82	54.42	53.59	45.18	44.72	43.31	42.99	52.63	54.36	55.40	47.52
TiO_2	0.00	0.00	0.44	0.00	0.43	0.00	0.00	0.53	2.03	2.42	2.63	2.71	0.50	0.42	0.20	0.77
Al_2O_3	3.38	2.43	2.80	2.92	2.37	3.48	2.64	1.34	9.18	9.90	11.90	11.94	2.93	1.88	0.87	5.80
FeO[a]	9.47	6.87	5.10	5.74	5.18	6.14	6.37	8.50	15.86	14.90	13.81	12.93	11.04	8.33	12.59	14.45
Cr_2O_3	0.00	0.00	0.32	0.00	0.42	0.00	0.00	0.20	0.00	0.00	0.00	0.00	0.00	0.00	0.00	0.00
MnO	0.00	0.00	0.35	0.00	0.34	0.00	0.00	0.35	0.22	0.20	0.20	0.19	0.34	0.26	0.37	0.37
MgO	13.18	14.23	17.48	16.76	17.97	16.24	16.31	16.56	12.76	13.10	13.25	13.55	17.70	18.88	16.10	15.36
CaO	23.57	23.66	19.52	19.58	19.54	19.33	18.88	18.52	11.12	11.31	10.88	11.02	11.47	12.44	12.36	9.94
Na_2O	0.00	0.00	0.54	0.51	0.51	0.00	0.70	0.42	1.98	2.11	2.19	2.17	0.69	0.51	0.35	1.37
K_2O	0.00	0.00	0.00	0.00	0.00	0.00	0.00	0.00	0.44	0.44	0.50	0.50	0.14	0.13	0.05	0.22
Total	99.99	100.00	99.98	100.01	100.00	100.01	99.32	100.01	98.77	99.10	98.67	98.00	97.44	97.21	98.29	95.80
Mg#	0.78	0.79	0.86	0.84	0.88	0.83	0.82	0.78	0.72	0.73	0.81	0.82	0.77	0.81	0.70	0.71
Cations are calculated on the basis of 6 O for clinopyroxene and 24 (O, OH, F) for amphibole																
Si	1.88	1.96	1.95	1.99	1.94	2.01	2.00	1.98	6.53	6.43	6.20	6.19	7.56	7.72	7.91	7.10
Ti	0.00	0.00	0.01	0.00	0.01	0.15	0.00	0.02	0.22	0.26	0.28	0.29	0.05	0.05	0.02	0.09
Al	0.15	0.10	0.13	0.12	0.10	0.00	0.11	0.05	1.56	1.68	2.01	2.03	0.50	0.31	0.15	1.02
Fe	0.17	0.21	0.16	0.18	0.16	0.19	0.20	0.27	1.92	1.79	1.65	1.56	1.33	0.99	1.50	1.81
Cr	0.00	0.00	0.01	0.00	0.01	0.00	0.00	0.01	0.00	0.00	0.00	0.00	0.00	0.00	0.00	0.00
Mn	0.00	0.00	0.01	0.00	0.01	0.89	0.00	0.01	0.03	0.02	0.02	0.02	0.04	0.03	0.05	0.05
Mg	0.73	0.79	0.95	0.91	0.97	0.00	0.90	0.91	2.75	2.81	2.83	2.91	3.79	4.00	3.43	3.42
Ca	0.94	0.94	0.76	0.77	0.76	0.76	0.74	0.73	1.72	1.74	1.67	1.70	1.77	1.89	1.89	1.59
Na	0.00	0.00	0.04	0.04	0.04	0.00	0.05	0.03	0.56	0.59	0.61	0.61	0.19	0.14	0.10	0.40
K	0.00	0.00	0.00	0.00	0.00	0.00	0.00	0.00	0.08	0.08	0.09	0.09	0.03	0.02	0.01	0.04
Sum	4.00	4.00	4.00	4.00	4.00	4.00	4.00	4.00	15.36	15.41	15.37	15.40	15.25	15.16	15.05	15.52

[a] Total Fe as FeO.

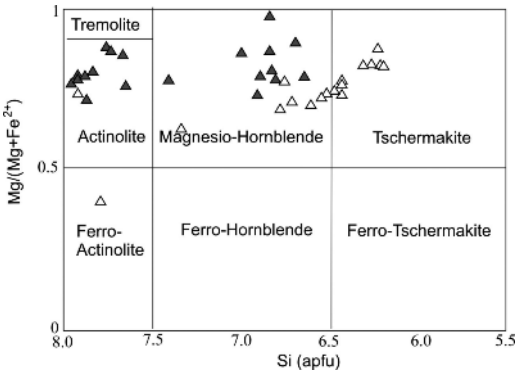

Figure 3. Calcic amphibole microprobe compositions from Serre dykes in Mg/(Mg+Fe^{2+}) vs Si (apfu) classification diagram (Leake et al., 1997). White triangles: A dykes; Dark grey triangles: F dykes.

between 0.91-2.33 wt.% and 0.00-2.17 wt.%, Na_2O between 1.69-2.02 wt.% and 0.00-2.16 wt.%, and K_2O between 0.41-0.90 wt.% and 0.00-0.54 wt.%, respectively. Tschermakite TiO_2 contents show a larger variation range (2.42-6.95 wt.%), as well as Na_2O (0.48-2.19 wt.%); K_2O show similar values (0.00-0.63 wt.%). Secondary amphibole has actinolite-Fe-actinolite (in A andesites) composition.

Feldspars

In group A dykes plagioclase phenocrysts show secondary albitic composition (An_{0-6}; Figure 4a; Table 2). Plagioclase of the groundmass mainly consists of albitic and rare unaltered labradoritic grains (An_{0-64}). Orthoclase ($Or_{86.2-98.0}$) is also present as microlites in the matrix. In group F dykes, plagioclase mainly shows albitic composition in both phenocrysts and groundmass; rare oligoclase occurs as microlites in the matrix (An_{0-25}; Figure 4b; Table 2). Very thin exsolution of K-feldspar (Or_{91-100}-Ab_{0-9}), optically undetectable, sometimes occur in the albite crystals. Pure orthoclase (Or_{100}) is also present in the groundmass. Plagioclase in ST dykes shows albitic composition with very low anorthite content (An_{0-5}; Figure 4c; Table 2). Potassium component is generally low ($Or_{0.6-2.9}$); only in few crystals, cores with higher Or component occur (Ab_{84-85}-Or_{14-15}; Table 2). Orthoclase is characterized by the absence or very low Ab contents (Ab_{0-11}-Or_{100-89}). Several attempts to obtain reliable compositional data on the feldspars from the VZ dykes resulted unsuccessful because of the pervasive alteration affecting these mineral phases in the studied rocks.

White mica

Textural and chemical criteria, as defined by Miller et al. (1981), allowed us to identify as magmatic only the white mica occurring in the ST (group II) samples. Texturally-defined primary muscovite, characterized by a coarser grain size and well-defined shapes, has higher Na and Ti and lower Si and Mg contents than secondary one. On the whole, primary white

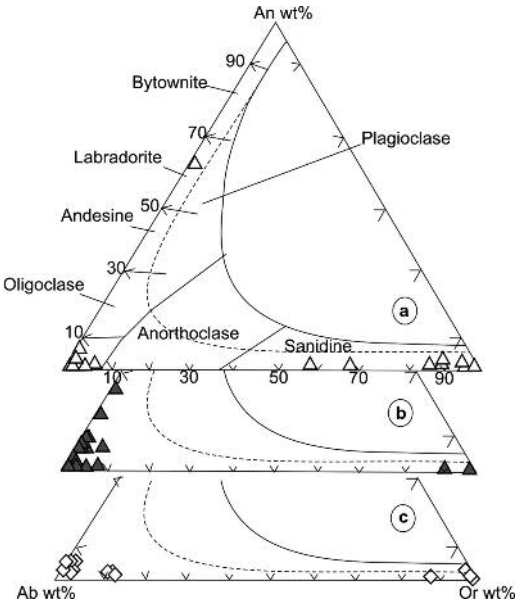

Figure 4. Feldspars compositions from Serre dykes in An-Ab-Or system. a = A samples; b = F samples; c = ST samples.

Table 2. Representative major element composition of feldspar from Serre dykes.

Sample	**A1a**			**A3c**		**F8**		**ST1**	**ST8**		
Location	gm	gm	gm	Ph r	Ph r	Ph c	gm	Ph r	Ph c	Ph c	Ph r
SiO_2	67.55	67.94	67.60	68.14	65.86	65.69	65.38	67.97	68.04	63.62	67.46
TiO_2	0.16	0.00	0.00	0.00	0.00	0.00	0.00	0.00	0.00	0.00	0.00
Al_2O_3	20.50	20.80	19.62	19.70	22.16	22.51	18.72	19.69	19.36	22.12	19.51
FeO[a]	0.58	0.32	0.16	0.15	0.00	0.00	0.00	0.06	0.19	0.52	0.21
MgO	0.20	0.13	0.66	0.61	0.00	0.00	0.00	0.70	0.75	0.93	0.72
CaO	1.11	1.13	0.26	0.32	1.30	1.41	5.88	0.03	0.14	0.12	0.22
Na_2O	9.88	9.68	11.57	10.99	10.67	10.40	10.02	11.45	11.37	10.16	11.50
K_2O	0.00	0.00	0.14	0.08	0.00	0.00	0.00	0.11	0.15	2.53	0.38
Total	99.98	100.00	100.01	99.99	99.99	100.01	100.00	100.01	100.00	100.00	100.00
Atomic proportions based on 32 O											
Si	11.80	11.83	11.85	11.90	11.54	11.50	11.63	11.88	11.91	11.33	11.84
Ti	0.02	0.00	0.00	0.00	0.00	0.00	0.00	0.00	0.00	0.00	0.00
Al	4.22	4.27	4.05	4.05	4.57	4.64	3.92	4.05	3.99	4.64	4.03
Fe	0.09	0.05	0.02	0.02	0.00	0.00	0.00	0.01	0.03	0.08	0.03
Mg	0.05	0.03	0.17	0.16	0.00	0.00	0.00	0.18	0.20	0.25	0.19
Ca	0.21	0.21	0.05	0.06	0.24	0.26	1.12	0.01	0.03	0.02	0.04
Na	3.35	3.27	3.93	3.72	3.63	3.53	3.46	3.88	3.86	3.51	3.91
K	0.00	0.00	0.03	0.02	0.00	0.00	0.00	0.03	0.03	0.58	0.09
Sum	19.73	19.66	20.10	19.94	19.98	19.94	20.13	20.04	20.04	20.39	20.13

[a] Total Fe is as FeO
Ph: Phenocryst; r: rim; c: core; gm: groundmass.

mica is here characterized by high Al_2O_3 (average value ~ 30.0 wt.%) and TiO_2 (0.8-0.9 wt.%) contents and K_2O and MgO values ranging between 9.7-10.4 wt.% and 1.3-1.7 wt.%, respectively (Table 3).

Whole-rock geochemistry

Major and trace element contents of representative samples are reported in Table 4. Most of them were affected by extensive post-magmatic alteration, partially responsible for the relatively high LOI contents (1.4-5.2 wt.%) and low CaO contents. The preferential mobility of alkalies compared to aluminium during hydrothermal stages, is likely responsible for the peraluminous character of many of these dykes [Aluminum Saturation Index (ASI) = molar $Al_2O_3/(CaO + K_2O + Na_2O)$ = 1.56-4.03], particularly evident in some alkali-poor VZ dykes (Table 4). In consideration of the widespread alteration, geochemical classification and modelling of the studied dykes has been essentially based on less mobile or immobile elements.

The SiO_2 content of the studied rocks ranges from ~ 56 to ~ 71 wt.%. According to the SiO_2 vs. Nb/Y classification diagram (Winchester and Floyd, 1977; Figure 5) group A and F dykes plot in the andesite field, whereas group ST and VZ dykes mostly plot in the dacite-rhyodacite field. The AFM diagram (Irvine and Baragar, 1971; Figure 6) suggests a calcalkaline affinity for all the investigated dykes. K_2O vs SiO_2 scheme (Peccerillo and Taylor, 1976) indicates a medium- to high-K calcalkaline composition

Table 3. Representative major element composition of muscovite from Serre dykes.

Sample	ST9	ST11	ST12
Location	gm	gm	gm
SiO_2	48.38	47.64	45.55
TiO_2	0.94	0.85	0.79
Al_2O_3	30.06	29.63	29.5
FeO[a]	3.04	3.41	5.5
MnO	0.04	0.00	0.02
MgO	1.29	1.31	1.7
CaO	0.02	0.04	0.07
Na_2O	0.12	0.14	0.13
K_2O	10.43	10.32	9.7
F	0.18	0.04	0.18
Total	94.50	93.38	93.14
Cations calculated on the basis of 24 (OH, F, Cl)			
Si	6.55	6.53	6.34
Ti	0.10	0.09	0.08
Al	4.79	4.78	4.84
Fe	0.34	0.39	0.64
Mn	0.01	0.00	0.00
Mg	0.26	0.27	0.35
Ca	0.00	0.01	0.01
Na	0.03	0.04	0.04
K	1.80	1.80	1.72
Sum	13.87	13.91	14.03

[a] Total Fe as FeO.

(Figure 7). Only the SiO_2-poor samples straddle the line dividing the tholeiitic and the medium-K calcalkaline fields. In these diagrams the composition of late- to post-Hercynian andesitic to rhyolitic calcalkaline dykes from Sardinia-Corsica Domain (SCD) is reported for comparison (Atzori and Traversa, 1986; Atzori et al., 2000; Traversa et al., 2003). A nearly complete overlap between the roughly coeval Serre and SCD dykes clearly emerges.

The group A and F andesites show a relatively high Mg#, ranging from 0.64 to 0.80 and from 0.66 to 0.76, respectively. Ni and Cr contents are high only in F samples (average values for Ni = 128 ppm and Cr = 250 ppm). Major and selected

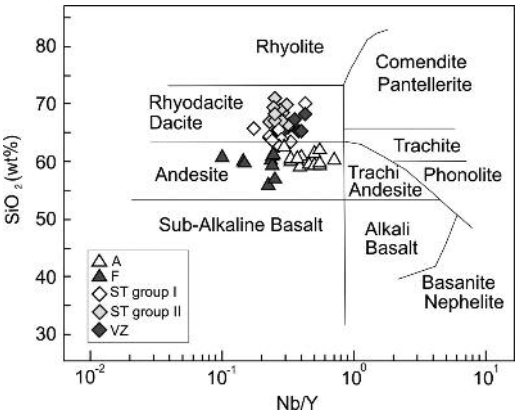

Figure 5. SiO_2 (wt.%) - Nb/Y (ppm) diagram (Winchester and Floyd, 1977). White triangles: A dykes; dark grey triangles: F dykes; white rhombs: ST silica-poor dykes (Group I); light grey rhombs: ST silica-rich dykes (Group II); dark grey rhombs: VZ dykes.

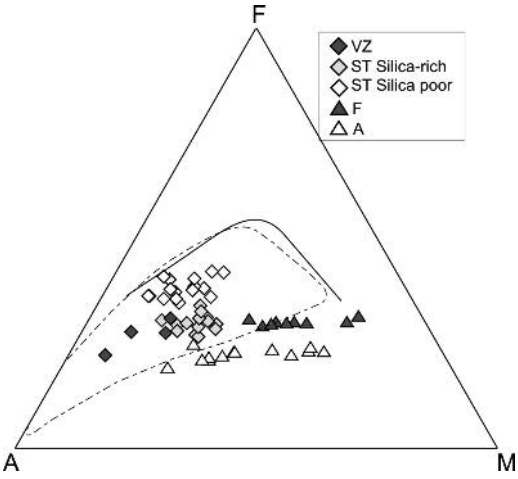

Figure 6. A (Na_2O+K_2O wt%) - F (FeO_{tot} wt%) - M (MgO wt%) diagram. Partition line is after Irvine and Baragar (1971). Dashed area includes calcalkaline post-Hercynian dykes of SCD (Atzori and Traversa, 1986; Atzori et al., 2000; Traversa et al., 2003). Symbols as in Figure 5.

Table 4. Major and trace element composition of selected Serre dykes.

Sample	Type	SiO_2	TiO_2	Al_2O_3	Fe_2O_3	MnO	MgO	CaO	Na_2O	K_2O	P_2O_5	LOI	Mg#	ASI	Cr	Ni	Rb	Y	Zr	Nb	Ba	Sr
A1b	A	60.26	0.45	12.77	4.8	0.13	9.77	2.69	2.76	1.78	0.17	4.41	80.1	1.8	256	102	65	9	157	3	311	170
A3d1	A	59.36	0.56	13.14	5.02	0.18	9.58	1.81	2.94	2.41	0.19	4.82	79.1	1.8	289	122	86	13	163	5	1004	173
A3c	A	61.72	0.62	15.35	3.79	0.09	4.8	1.88	4.61	3.38	0.22	3.53	71.5	1.6	60	25	119	10	126	5	515	189
A1e	A	60.64	0.6	16.76	3.43	0.09	4.15	2.6	3.01	3.92	0.2	4.59	70.6	1.8	16	10	164	10	181	7	384	146
A3d2	A	59.81	0.57	14.31	4.6	0.14	8.48	1.6	3.25	2.6	0.19	4.44	78.5	1.9	222	85	85	13	165	6	706	173
A1a	A	59.69	0.5	13.88	5.02	0.15	9.13	2.23	2.3	2.68	0.18	4.23	78.3	1.9	287	103	112	10	165	5	632	291
F4	A	59.67	0.52	13.49	6.02	0.12	7.67	2.54	2.96	1.91	0.19	4.91	71.6	1.8	288	138	85	20	157	5	190	114
F5	A	60.43	0.52	13.33	5.80	0.12	7.14	2.99	3.27	1.73	0.20	4.47	70.9	1.7	283	137	63	19	144	3	221	184
F6	A	56.19	0.63	13.63	8.20	0.12	12.89	0.34	2.43	0.61	0.19	4.77	75.7	4.0	299	139	30	18	158	4	38	39
F7	A	57.27	0.61	13.61	7.34	0.12	11.69	0.72	2.77	0.78	0.19	4.92	76.0	3.2	299	140	37	19	161	5	83	75
F8	A	59.99	0.52	13.12	6.10	0.19	8.25	3.13	3.12	1.38	0.20	4.01	72.9	1.7	290	173	51	21	148	3	207	192
VZ1	D	67.45	0.24	17.38	2.32	0.06	0.76	2.49	0.04	4.61	0.09	4.55	39.5	2.4	2	3	248	26	188	9	355	25
VZ2	D	65.37	0.24	18.24	3.07	0.11	1.48	1.88	0.05	4.60	0.10	4.86	48.8	2.8	3	3	242	24	187	9	193	16
VZ4	D	68.33	0.25	20.22	1.82	0.01	0.56	0.26	0.04	5.14	0.11	3.27	37.8	3.7	4	2	260	26	191	10	175	15
ST1	D-RD s-p	65.90	0.70	15.20	5.56	0.10	1.31	1.98	4.43	2.97	0.23	1.61	31.9	1.6	bdl	3	119	36	274	11	463	220
ST3	D-RD s-p	63.43	0.81	15.01	6.92	0.11	3.27	0.79	4.12	2.68	0.23	2.64	48.3	2.0	2	4	111	38	289	12	362	147
ST4	D-RD s-p	67.08	0.63	14.69	5.41	0.09	1.27	1.95	5.47	1.81	0.23	1.38	31.7	1.6	1	4	57	33	266	11	377	179
ST5	D-RD s-p	65.44	0.65	14.81	6.60	0.11	1.77	1.62	4.72	2.33	0.24	1.71	34.7	1.7	3	5	81	41	271	11	497	169
ST8	D-RD s-r	69.97	0.20	15.50	3.40	0.02	2.68	0.14	2.89	2.66	0.06	2.47	61.0	2.7	9	4	154	29	167	9	156	68
ST9	D-RD s-r	70.97	0.19	14.83	3.24	0.02	2.68	0.11	2.82	2.51	0.05	2.58	62.1	2.7	10	4	146	29	160	7	145	63
ST10	D-RD s-r	70.19	0.22	15.63	3.48	0.03	2.18	0.11	3.20	2.64	0.06	2.27	55.4	2.6	10	3	136	26	195	11	135	67
ST11	D-RD s-r	67.06	0.38	16.24	4.00	0.04	2.90	0.28	3.46	2.44	0.11	3.09	59.0	2.6	10	5	114	25	217	7	216.	86
ST12	D-RD s-r	67.02	0.38	16.36	4.42	0.04	2.92	0.25	3.26	2.60	0.10	2.65	56.7	2.7	9	5	115	24	220	7	223	96
ST13	D-RD s-r	65.73	0.38	16.69	4.69	0.05	3.27	0.29	3.43	2.59	0.11	2.78	58.0	2.6	8	4	116	27	227	7	235	107
ST14	D-RD s-r	65.61	0.39	16.46	4.50	0.04	3.67	0.26	3.22	2.69	0.09	3.08	61.8	2.7	11	3	114	25	226	7	215	85
ST15	D-RD s-r	66.36	0.39	16.52	4.46	0.04	3.28	0.26	3.19	2.78	0.10	2.63	59.3	2.6	10	5	121	23	227	7	212	83
ST17	D-RD s-r	66.91	0.39	16.53	4.37	0.04	2.86	0.25	3.25	2.62	0.10	2.68	56.5	2.7	10	6	116	23	216	5	227	79
ST18	D-RD s-r	68.02	0.37	15.32	4.79	0.06	2.71	0.37	2.88	2.78	0.11	2.60	52.8	2.5	bdl	4	119	24	202	6	217	71
ST25	D-RD s-p	65.71	0.63	14.17	7.00	0.09	3.38	0.51	2.38	2.97	0.18	2.98	48.9	2.4	7	4	111	27	170	13	382	73
ST26	D-RD s-p	65.50	0.66	15.31	6.30	0.08	1.43	1.09	4.00	2.75	0.23	2.67	31.0	2.0	bdl	2	118	41	265	11	429	138
ST27	D-RD s-p	63.85	0.76	15.50	6.49	0.10	2.67	0.69	4.23	2.34	0.25	3.13	45.0	2.1	3	5	94	35	266	10	474	122
ST28	D-RD s-p	62.85	0.81	16.25	6.92	0.12	2.60	0.84	3.53	3.01	0.25	2.83	42.7	2.2	bdl	5	131	46	290	12	516	203
ST29	D-RD s-p	64.14	0.73	15.59	5.97	0.11	2.09	1.55	3.61	3.32	0.24	2.67	41.0	1.8	2	5	126	37	257	9	519	196
ST30	D-RD s-p	64.14	0.72	15.23	6.37	0.11	2.72	1.28	4.34	2.35	0.24	2.51	45.8	1.9	bdl	5	97	38	260	8	364	147

A: andesite; D: Dacite; D-RD: dacite-rhyodacite; s-p: silica poor; s-r: silica rich; LOI = Weight loss on ignition;
ASI = Alumina Saturation Index [molar Al/(Ca+Na+K)]; bdl = below detection limit.

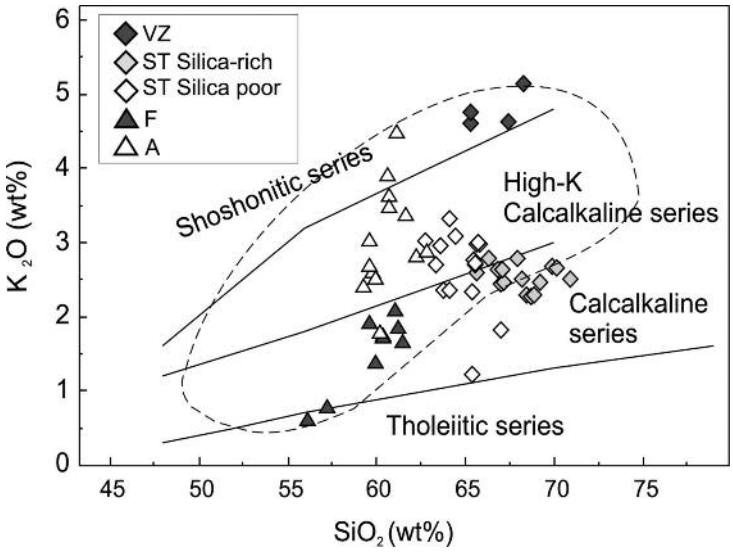

Figure 7. K_2O (wt%) vs SiO_2 (wt%) (Peccerillo and Taylor, 1976). Area as in Figure 6. Symbols as in Figure 5.

trace element variations are shown in Figures 8-9 and reported in Table 4. As a general trend, the dykes show a clear negative correlation with silica only for MgO and Fe_2O_3, whereas the rest of the major oxides show complex or absent correlations. The ST group is characterized by higher Fe_2O_3 compared to the rest of the sample groups for a given SiO_2 content. Another interesting feature is the common distinction of the ST dykes into two main groups, one relatively SiO_2-poor (characterized by relatively low MgO and high Fe_2O_3, TiO_2, P_2O_5, CaO and, less clear, Na_2O) and the other relatively SiO_2-rich. No substantial differences between the SiO_2-rich and SiO_2-poor ST sub-groups can be observed for K_2O. This geochemical distinction in two sub-groups reflects that already highlighted by the petrographic investigations.

The Serre dykes show complex correlations of trace elements with SiO_2 (Figure 9 and Tables 4, 5). Large Ion Lithophile Elements (LILE) are quite scattered, only Rb showing a slight positive correlation with SiO_2 in A, F and ST samples. Group F andesitic dykes show positive correlation between LILE and SiO_2, while group A andesites show absent or even negative correlation. The andesites, as a whole group, show lower High Field Strength Element (HFSE; Nb, Hf, Zr) and higher transition element content (Ni, Cr, Sc, V, Co) than dacitic and rhyodacitic dykes. HFSE, Y and Rare Earth Elements (REE) contents in the andesitic dykes are not correlated with SiO_2, differently from what observed for dacites and rhyodacites that show a roughly negative correlation, at least for HFSE. Despite scattering, the observed variation trends are on the whole compatible with the existence of genetic links between samples of the same dyke group, but speak against substantial genetic relationships between the different dyke groups.

Major and trace element compositions of the Serre dykes are compared with those of SCD dykes (Atzori and Traversa, 1986; Atzori et al., 2000; Traversa et al., 2003) and Serre metaluminous to strongly peraluminous granitoids (Rottura et al., 1990). The greatest differences are

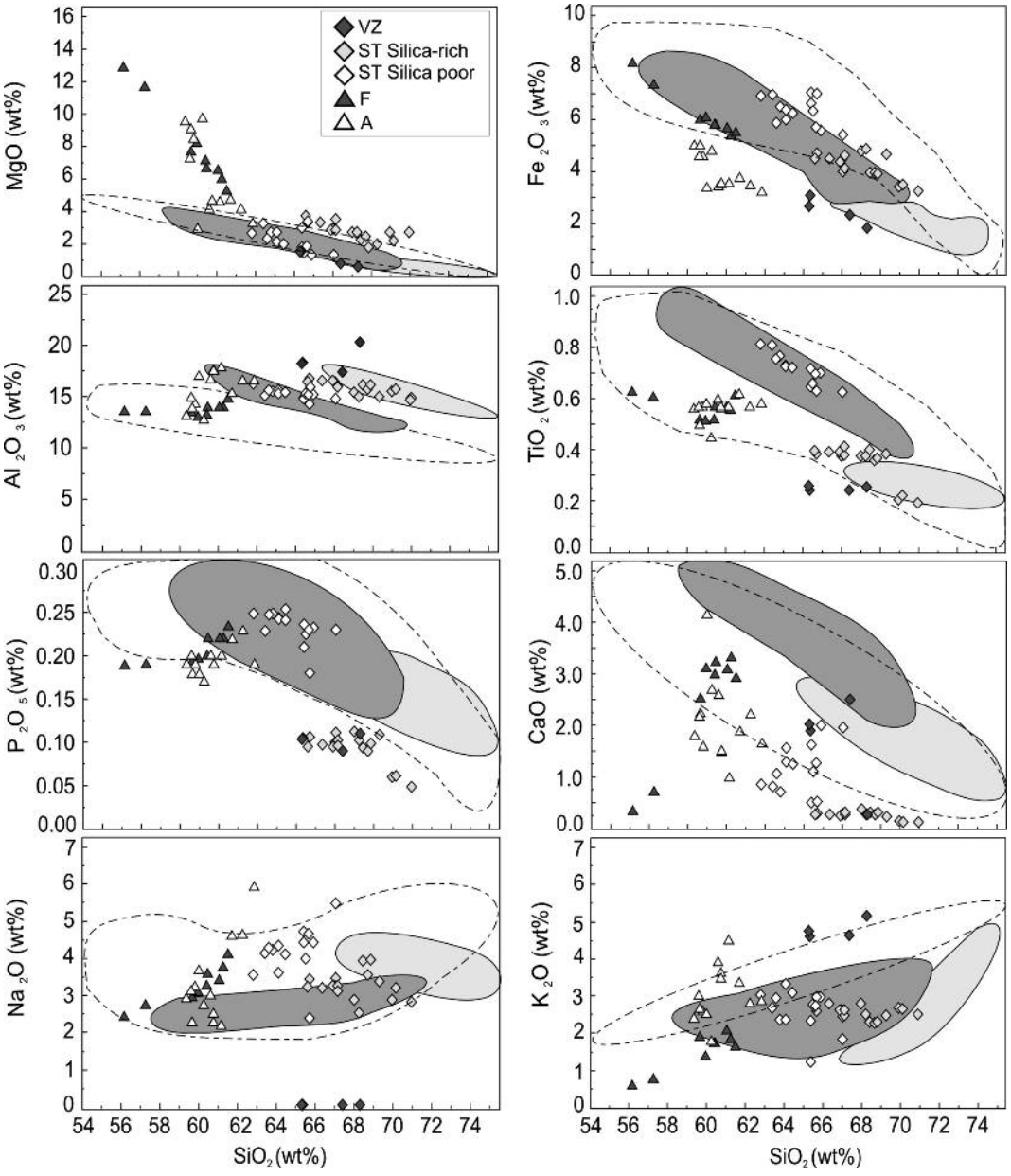

Figure 8. Major element contents (wt.%) vs SiO_2 (wt.%) diagrams. Dashed area: post-Hercynian calcalkaline dykes of the SCD (Atzori and Traversa, 1986; Atzori et al., 2000; Traversa et al., 2003); grey and light grey areas: calcalkaline metaluminous and strongly peraluminous granitoids of Serre Massif, respectively (Rottura et al., 1990). Symbols as in Figure 5.

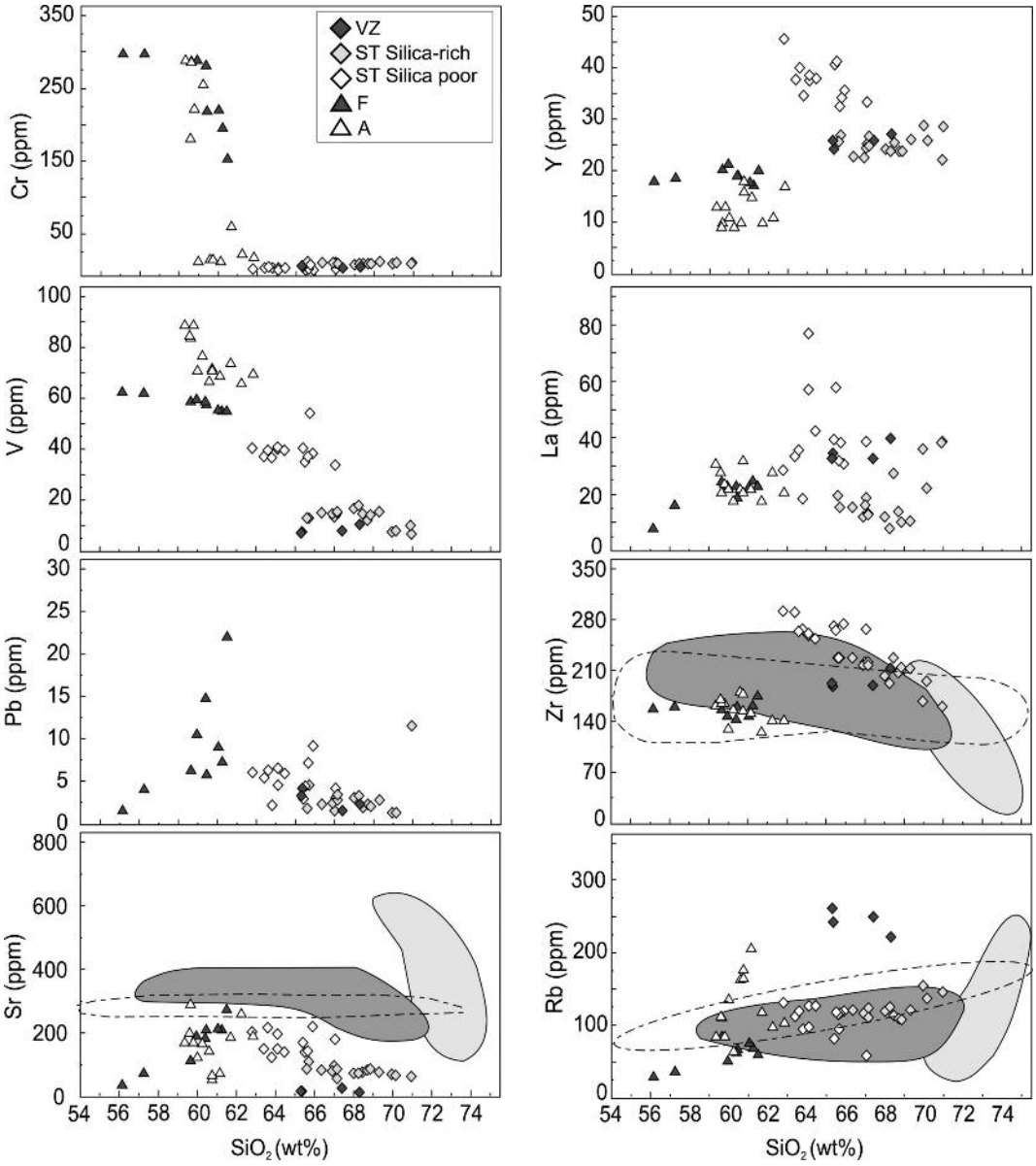

Figure 9. Selected trace element contents (ppm) vs. SiO_2 (wt.%). Dashed area: post-Hercynian calcalkaline dykes of the SCD (Atzori and Traversa, 1986; Atzori et al., 2000; Traversa et al., 2003); grey and light grey areas: calcalkaline metaluminous and strongly peraluminous granitoids of Serre Massif, respectively (Rottura et al., 1990). Symbols as in Figure 5.

Table 5. Additional trace element analyses by ICPMS of selected Serre dykes.

Sample	La	Ce	Nd	Sm	Eu	Tb	Yb	Lu	Th	U	Ta	Hf
A1b	18.0	40.0	20.4	3.9	1.0	0.5	1.3	0.2	7.1	1.9	0.5	4.0
A3c	18.0	57.0	22.6	4.2	1.2	0.5	1.3	0.2	7.6	2.2	0.5	4.0
A1e	22.0	53.0	21.9	4.2	1.2	0.5	1.3	0.2	7.9	2.1	0.5	4.0
A3d2	24.0	34.0	24.6	4.6	1.2	0.6	1.3	0.2	7.4	2.4	0.5	4.0
A1a	18.0	29.0	20.6	3.9	1.0	0.5	1.3	0.2	7.2	2.0	0.5	4.0
F4	24.6	54.4	21.3	4.2	1.5	0.5	1.3	0.3	7.1	2.0	0.5	4.0
F5	23.1	41.0	20.8	4.2	1.1	0.6	1.4	0.2	7.0	2.1	0.5	3.0
F8	23.2	44.2	23.6	4.9	1.3	0.7	1.8	0.3	7.3	2.3	0.5	3.0
VZ1	52.9	59.8	34.0	6.3	1.0	0.8	2.1	0.3	16.9	4.1	0.7	5.0
VZ2	32.5	59.5	35.0	6.7	1.0	0.9	2.1	0.3	16.8	4.4	0.8	5.0
VZ4	39.4	67.5	38.2	7.0	1.0	0.8	2.2	0.3	18.2	5.0	0.8	6.0
ST4	38.3	81.2	36.9	7.6	1.6	1.0	2.8	0.4	10.8	2.4	0.5	6.0
ST5	39.1	81.1	37.5	7.6	1.7	1.1	3.0	0.5	10.3	2.6	0.5	6.0
ST9	38.3	87.7	35.4	6.7	1.1	1.0	2.6	0.4	14.2	3.1	0.6	5.0
ST10	21.9	50.5	21.7	4.6	0.8	0.8	2.7	0.4	14.4	3.4	0.6	5.0
ST11	18.6	26.1	13.7	3.1	0.7	0.6	2.0	0.4	8.2	2.8	0.5	5.0
ST12	15.9	20.4	10.5	2.5	0.6	0.5	2.0	0.3	8.2	2.9	0.5	5.0
ST13	15.1	16.8	9.7	2.5	0.6	0.5	2.2	0.4	8.6	3.0	0.5	5.0
ST17	12.0	30.4	14.9	3.0	0.6	0.5	1.9	0.3	8.2	2.8	0.5	5.0
ST26	57.6	91.8	46.5	8.6	1.8	1.2	3.1	0.5	11.5	2.9	0.5	6.0
ST27	18.1	35.4	18.9	4.2	0.8	0.7	3.4	0.6	10.7	3.0	0.5	6.0
ST28	28.2	49.9	25.9	5.8	1.1	1.0	3.6	0.6	11.4	3.4	0.6	6.0
ST30	76.8	187.6	67.3	11.3	2.3	1.4	3.2	0.6	11.0	2.8	0.5	6.0

seen in the anomalously high MgO and low Al_2O_3 content of the Serre dykes, which are also characterized by low to very low Ca content at any SiO_2 value (Figure 8), all largely reflecting the effects of post-magmatic alteration. Group VZ dykes and SiO_2-rich group ST dykes are also characterized by anomalously low P_2O_5 content. The ST dacitic-rhyodacitic dykes, intruding the metaluminous to weakly peraluminous Serre granitoids, show a rough similarity with these rocks.

Chondrite-normalized REE patterns (Figure 10) are weakly to strongly fractionated, with La_N/Yb_N ratios ranging from 9.9 to 14.0 and from 8.5 to 11.8 for group A and F andesites, respectively. Europium anomaly ranges from slightly negative to slightly positive values (Eu/Eu* = 0.82-1.21). The VZ dacitic samples show REE fractionation similar to that of the andesites (La_N/Yb_N = 12.9-13.8), but with a more prominent Eu negative anomaly (Eu/Eu* ~ 0.53). On the other hand, the ST dacitic and rhyodacitic samples show a much more variable REE fractionation (La_N/Yb_N = 2.6-16.3), coupled with clear Eu negative anomaly (Eu/Eu* = 0.53-0.83). The VZ dykes show nearly flat HREE patterns, with Ho_N/Lu_N ratios ranging from 0.95 to 1.71. HREE are nearly constant also in the other dyke groups, clustering around 4-9 times CI chondrite for the andesites, around 10 times for the VZ dacites and around 10-20 times for the ST dacites and rhyodacites.

On the whole, REE element patterns of the Serre dykes share many similarities with the late- to post-tectonic granitoids of the Serre batholith and with the post-Hercynian intermediate to felsic dykes from the SCD (Figure 10).

Primitive mantle-normalized incompatible element patterns (Figure 11) show some common features, i.e., LILE enrichment relative to HFSE, peaks at Rb and Pb, negative anomalies at Ba, Nb-

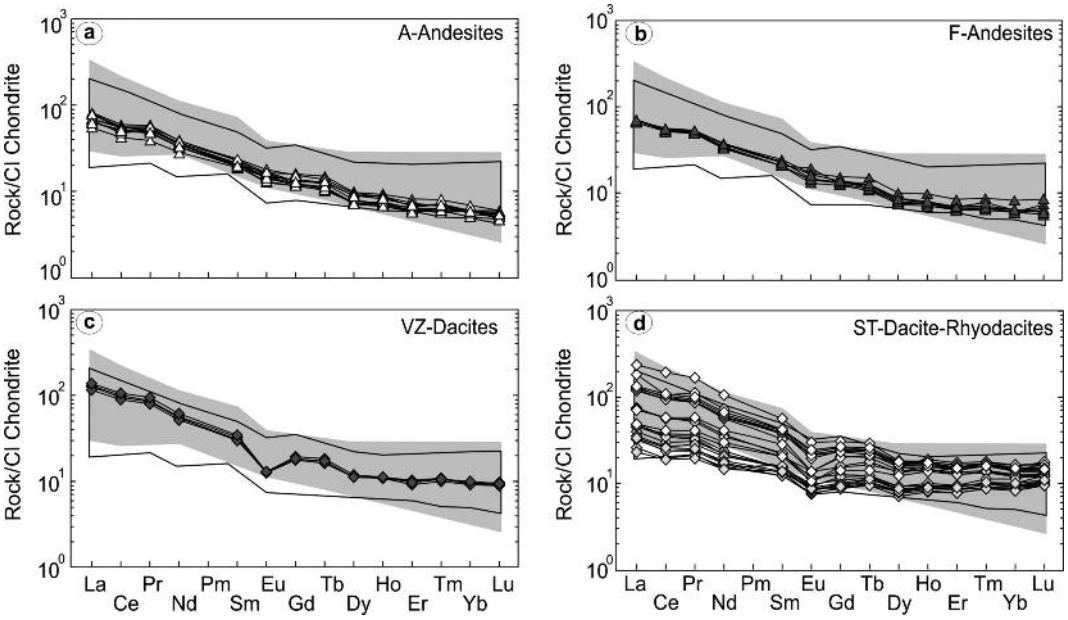

Figure 10. Chondrite CI-normalized REE patterns for the Serre dykes: a) A samples; b) F samples; c) VZ samples; d) ST samples. Normalization after Nakamura 1974. White area: SCD calcalkaline dykes (Atzori and Traversa, 1986; Atzori et al., 2000; Traversa et al., 2003); grey area: Serre calcalkaline granitoid rocks (Rottura et al., 1990).

Ta, Ti and Sr. Compared with the andesitic rocks, dacitic and rhyodacitic samples show stronger Ba, Sr and Ti negative anomalies and a less pronounced peak at Pb, but overall similar patterns. On the whole, these patterns show typical features of subduction-related magmas (Figure 11; Shimizu and Arculus, 1975; Pearce, 1983; Lustrino et al., 2011).

Discussion

Minero-petrographic and geochemical features suggest, on the whole, an origin from mantle sources modified by fluids produced by metamorphic dehydration reactions during subduction of oceanic slabs for the Serre dykes. The absence of iron enrichment in the first evolutionary stages is probably the strongest evidence for their calcalkaline character (e.g., Arculus, 2003). This, coupled with low TiO_2 and relatively low alkali contents resemble closely the chemical composition of magmas emplaced along active or fossil subduction zones (e.g., Lustrino et al., 2011, and references therein). Unlike typical arc-type rocks, the Serre dykes display a distinct Ba negative anomaly with respect to the adjacent Rb and Th. This trough can be considered not related to the alteration processes but a consequence of crystal fractionation or distinctive source characteristics. This feature also occurs in Plio-Quaternary potassic to ultrapotassic subduction-related rocks from peninsular Italy (Peccerillo and Martinotti, 2006; Avanzinelli et al., 2009; Conticelli et al., 2010 and references therein). Among the incompatible trace elements, the HFSE troughs, the positive Pb anomaly and the high LILE/HFSE ratios are classically considered as

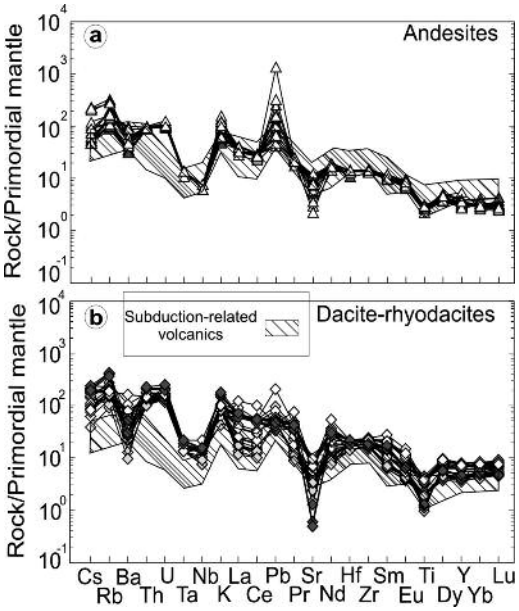

Figure 11. Primitive mantle normalized trace elements patterns for Serre calcalkaline dykes: a) A and F samples; b) ST and VZ samples. Normalization after McDonough and Sun, 1995. Data field for subduction-related volcanic is shown for comparison (Gerlach et al., 1988).

typical features of subduction-related igneous rocks (Gill, 1981; Grove and Kinzler, 1986; Tatsumi, 1989; Davies and Stevenson, 1992; Hawkesworth et al., 1993; Arculus, 1994; Pearce and Peate, 1995) These characteristics have been commonly explained by the addition of hydrous fluids released from subducting oceanic lithosphere, selectively enriched in LILE and in other fluid-mobile elements (e.g., Pb, U, with high to very high Pb/U ratios), to the mantle wedge, lowering the mantle solidus and leading to magma generation.

The occurrence of such subduction-related geochemical characteristics is at odd with the envisaged tectonic setting of the emplacement of the dykes, being these emplaced after the end of the Gondwana-Laurasia collision (e.g., Stampfli and Borel, 2002). A general agreement exists that late-Hercynian Calabrian magmas were emplaced in an extensional tectonic setting associated with the post-collisional attenuation of the previously thickened lithosphere in consequence to possible slab detachment (Caggianelli et al., 2007 and references therein). Calcalkaline magma with geochemical features similar to those observed in the intermediate Serre dykes can be produced by decompression melting of an asthenospheric mantle source previously metasomatized by subduction-related fluids/melts (Johnson et al., 1978; Cameron et al., 2003) or of a continental lithospheric mantle previously modified by subduction (Hawkesworth et al., 1995; Wilson et al., 1997). Besides, calcalkaline compositions have been interpreted in literature also as the effect of the interaction between mantle-derived melts with local crust, through wall-rock assimilation and fractional crystallization (Stille and Buletti, 1987; Innocenti et al., 1994; Rottura et al., 1998; Cannic et al., 2002). In all these cases, the presence of calcalkaline magmatism does not automatically imply the presence of coeval subduction. In the next paragraph, we therefore investigate the possible petrogenetic models that may better explain the intermediate-felsic calcalkaline dyke magmatism in the Serre Massif.

Petrogenetic model

In the Th/Yb vs. Ta/Yb discrimination diagram for intermediate-felsic rocks (Pearce, 1983; Gorton and Schandl, 2000; Figure 12a), the Serre andesitic dykes plot in the active continental margin field together with most of the ST silica-rich dacite-rhyodacites. The other dacite-rhyodacitic samples straddle the boundary with the volcanic arc field (Figure 12a). Similar considerations can be made using the Rb vs Y+Nb discrimination diagram for felsic compositions (Pearce et al., 1984; Figure 12b), where the Serre dacites and rhyodacites mainly plot in the Volcanic Arc Granites field

(VAG) field, which also includes Active Continental Margin Granites, and near the triple point, as commonly observed for post-collisional granitic rocks (Pearce, 1996).

Dykes with andesitic composition crop out in two localities: Foletti Valley (F group) and Antonimina (A group). The dykes of these two areas share many petrographic similarities but can be easily distinguished geochemically, being the group F andesites characterized by much higher Fe_2O_{3tot} (5.40-8.20 wt.%) and lower K_2O (0.61-2.09 wt.%) than group A andesites (3.22-5.02 wt.% and 1.78-4.50 wt.% for Fe_2O_{3tot} and K_2O, respectively; Figure 8). With the exception of the andesites with the lowest SiO_2 content, the group F andesites have also typically higher CaO than group A dykes (Figure 8). On the other hand, the two types of andesites cannot be distinguished on the basis of the compatible and incompatible trace element content (Figures 9, 11a). This feature is at odd with what observed for major elements and leads to hypothesize that the Fe, K and Ca differences between the two groups are not necessarily primary features, but have been possibly acquired during post-magmatic alteration of the rock. Weathering of feldspars, amphibole and other mafic phases at different degrees may result in inter-element fractionation of these three elements, resulting in the apparently distinct liquid lines of descent observed in Figure 8.

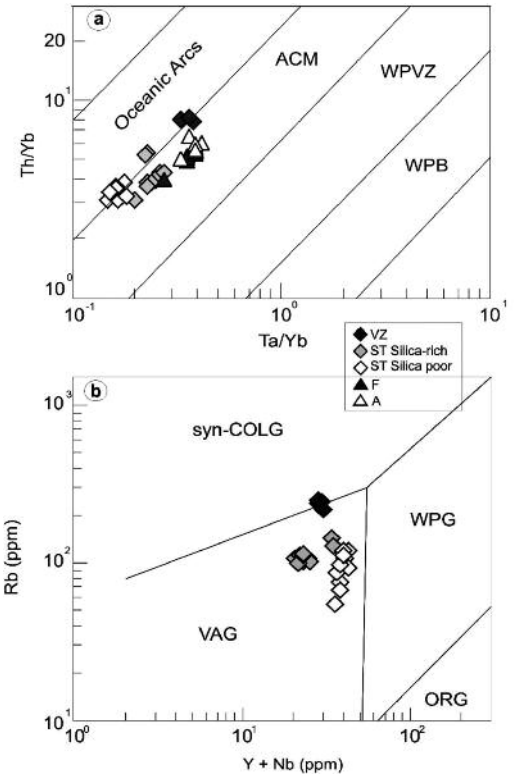

Figure 12. a) Compositions of Serre dykes in the Th/Yb vs. Ta/Yb plot (Pearce, 1983) modified by Gorton and Schandl (2000) for intermediate-felsic rock compositions. Oceanic Arcs; ACM: Active Continental Margins; WPVZ: Within Plate Volcanic Zones; WPB: Within Plate Basalts. b) Rb (ppm) vs. Y+Nb (ppm) diagram (Pearce et al., 1984) for Serre dacite-rhyodacitic dykes. SYN-COLG: syn-collisional granites; WPG: within-plate granites; VAG: volcanic arc granites; ORG: ocean-ridge granites.

As a whole, andesitic dykes are too much enriched in Mg#, for a given SiO_2 content, to be interpreted as partial melts of crustal rocks. Their high Mg# (0.64-0.80) is likely the result of the replacement of clinopyroxene by high-MgO chlorite. The Serre andesites show features related to the interaction between mantle-derived magmas which have variably interacted with crustal components, as reflected by variable LREE/HFSE (e.g., La/Nb = 2-13) and LILE/HFSE (e.g., Ba/Nb = 9-200) ratios. These variations might be caused by either magma mixing, crustal contamination as well as by concurrent assimilation and fractional crystallization (AFC; De Paolo, 1981). What now must be established is to understand if the interaction with crustal rocks (typically characterized by low HFSE, high LILE, high LILE/HFSE and high Pb; e.g., Rudnick and Gao, 2004, and references therein) did happen at mantle depths (e.g., after recycling of crustal rocks along subduction zones) or at crustal depths, during

interaction of mantle melts with crustal lithologies (e.g., in magma chambers, via AFC processes).

To better understand the mechanisms that originated the two groups of intermediate Serre dykes, FC, AFC and mixing calculations have been carried out, by using the FC-AFC-FCA and mixing modeller program of Ersoy and Helvaci (2010). Results confirm that a single evolutionary trend for both andesite groups is very unlike. Indeed, in the Sr/Y vs. Y diagram (Figure 13a) calculations performed with A1a sample chosen as starting composition, indicate that the A andesites are genetically related each other by fractional crystallization (black solid line) of ~ 20% clinopyroxene, ~ 20% amphibole and ~ 60% plagioclase, starting from the average modal proportion of the most primitive sample. On the contrary, most of the F samples plot on the trajectory depicting mixing processes (black dotted line) between A1a-like parent magma and melts deriving from melting of Calabrian lower crustal metapelites (LCM; Del Moro et al., 2000; Figure 13a), now exposed in the northern sector of the Serre Massif. However, other samples of the F group do not plot along well defined trends, possibly reflecting variable interplay of mixing and FC-AFC processes, as well as possible minor alteration effects. The same calculations were replicated, considering F andesitic rocks as a separate population and F3 sample as the starting composition (Figure 13a). The modeled mixing curve (grey dotted line) nearly retraces the previous mixing trend, but in this case, simple fractionation (FC; grey solid line) from the more primitive F andesites appears to be the process more appropriate to explain compositions of the samples plotting out of the mixing trend. In addition, in the Ba/Nb vs. La/Nb diagram (Figure 13b), F dykes clearly separate from A ones, showing an AFC-mixing trend that seems to exclude any genetic link between the two dyke populations and highlights, instead, a significant contribution of crustal components, either as rock-contaminant and/or crustal melt in the generation of the F dykes. Alternatively, the Ba/Nb vs. La/Nb plot can be interpreted in a different way: elements resistant to post-magmatic hydrothermal alteration (e.g., REE and HFSE) are similar in the two groups (F and A dykes have overlapping La/Nb), with the most important differences seen only when elements mobile in fluid phases (e.g., LILE) are compared to relatively immobile elements (HFSE). According to this view, the different Ba/Nb could be also interpreted as the secondary effect of weathering, more evident in the A dykes than in the F samples. The overlapping Cr and Ni content of the two andesitic rock groups can be considered as a proof that substantial assimilation

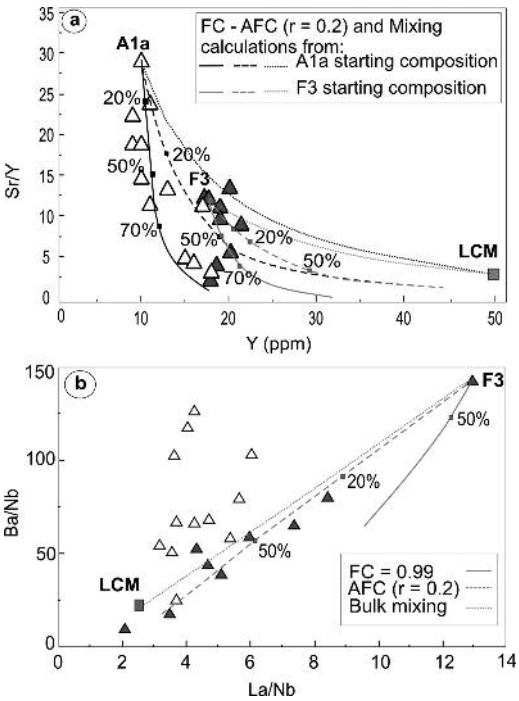

Figure 13. a) Sr/Y vs. Y and b) Ba/Nb vs. La/Nb diagrams for Serre andesitic rocks. Black lines refer to A samples, grey lines refer to F samples. Serre lower crust metapelites (LCM; average composition) are from Del Moro et al., 2000. A1a - F3: starting composition. r = assimilation/fractionation ratio.

did not occur, because this would have caused cooling of the hybrid magma with the following increase of fractional crystallization of Ni-Cr-rich mafic phases (e.g., olivine and pyroxenes).

Nevertheless, the high Ba/Nb (25-201), La/Nb (3.1-6.2) and Th/La (0.25-0.42) and the low Nb/La (0.16-0.32) ratios of the A group dykes are a clear evidence of involvement of crustal lithologies in the genesis of these samples. However, the straightforward results of the geochemical modeling indicate that simple fractional crystallization from a A1a-like parent magma may be considered the main petrogenetic process for these andesites.

FC-AFC calculations have been carried out also for the dacite-rhyodacite dykes. Results (not shown) suggest the absence of fractional crystallization links with the andesitic melts. The geochemical similarities between the felsic dykes and the Serre granitoids can be interpreted hypothesizing that the high-K felsic volcanic rocks are related to partial melting of crustal rocks (e.g., von Blanckenburg et al., 1998; Altherr et al., 2000; Altherr and Siebel, 2002). At this purpose, crustal involvement in the origin of dacitic and rhyodacitic compositions is investigated using the results of dehydration melting experiments of different crustal rocks, such as amphibolites, tonalitic gneisses, metagreywackes and metapelites, under variable melting conditions (Altherr and Siebel, 2002 and references therein). In Figures 14a-b, ST dacitic-rhyodacitic compositions are broadly compatible with an origin by melting of a metapelitic source. Nevertheless, these diagrams highlight the already reported separation in the two sub-groups of silica-poor and silica-rich ST samples, suggesting a derivation from different crustal sources. A metapelitic crustal source appears to be likely for the silica-rich magmas, while a two-components metapelitic-metabasaltic sources seems to have been involved in the genesis of the silica-poor ST dykes.

Moreover, in ST silica-poor samples, Na_2O contents and Mg# values are respectively higher and lower than those from silica-rich samples, consistent with the assumption that partial melts from metabasaltic sources are generally characterized by higher contents of Na_2O and lower values of Mg# than melts from other sources (Rapp and Watson, 1995 and references therein). Additionally, the distinct petrographic features observed in ST silica-rich samples (e.g., presence of magmatic white mica), also support a different genetic mechanism.

The composition of group VZ dacitic dykes appears consistent with the derivation from a metapelitic crustal source in the Mg# vs. SiO_2 diagram (Figure 14a), whereas in the Al_2O_3/(MgO + FeO) vs CaO/(MgO+FeO) diagram (Figure 14b), VZ samples show a very scattered distribution that can be hardly related to a pure metapelitic crustal source composition. Nevertheless, even considering the alteration effects, the composition of the dacites could results from hybridization of mantle derived melts with metapelites. Such mixing processes between crustal- and mantle-derived melts appear consistent with the "disequilibrium" textures observed in the VZ dacitic rocks (mantled feldspar phenocrysts, quartz *ocelli* and dissolution textures).

Conclusions

Post-collisional magmatic dykes, intruding metamorphic basement rocks as well as late Hercynian granitoids in four different areas of the Serre Massif, southern Calabria-Peloritani Orogen, range in composition from andesites (A-F groups) to dacites-rhyodacites (VZ-ST groups), all showing a medium- to high-K calcalkaline affinity. The two groups of andesites show subtle major element differences (mostly Fe, Ca, and, in a lesser amount, Al and K) that can be alternatively interpreted as different parental magma compositions or, more likely, as secondary effects due to the diffuse post-

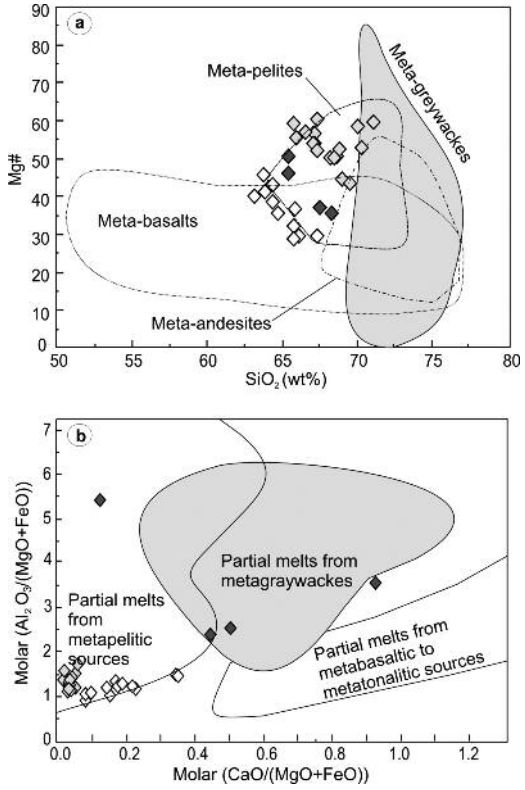

Figure 14. Composition of Serre dacite-rhyodacites compared with composition of partial melts obtained in experimental studies by melting of various crustal rocks. a) SiO_2 vs. Mg# diagram. b) molar CaO/(MgO + FeO) vs. molar Al_2O_3/(MgO + FeO) diagram. (Altherr and Siebel, 2002, and references therein).

magmatic weathering. Relatively immobile incompatible and compatible trace element content and ratios of the two andesite dyke groups are very similar, the only differences being found only for relatively mobile incompatible trace elements (e.g., LILE). These features can be interpreted as evidence of crustal contamination at shallow depths starting from a similar source or, more likely, as post-magmatic elemental mobility.

Two sub-groups of silica-rich and silica-poor rocks, have been detected among the ST dacite-rhyodacite samples, that define separate behaviours in variation trends, reflecting further different petrogenetic mechanisms.

All the intermediate-felsic Serre dykes show typical subduction-related geochemical signatures, as typically found in other post-collisional igneous rocks of the European Hercynian Belt. On the whole, the studied calcalkaline dykes, intruding Hercynian phyllites and late-Hercynian undeformed granitoid rocks, were likely generated in a post-collisional extensional context, characterized by lithosphere thinning promoting upwelling of hot asthenosphere. This is indeed the general framework envisaged for dykes of roughly similar composition widespread in western Europe, such as those from the Sardinia-Corsica Domain (Atzori and Traversa, 1986; Atzori et al., 2000; Traversa et al., 2003), for which a transition from a compressive to extensional geodynamic setting has been invoked to explain their geochemical features. Calcalkaline affinity and geochemical signatures of such post-collisional rocks have been interpreted as a result of variable crustal contamination of mantle magmas derived from subduction-modified lithospheric and/or asthenospheric mantle sources.

Geochemical compositions of Serre andesitic dykes (A and F groups), including relatively high Mg# values and MgO, Ni and Cr contents, as well as variable LREE/HFSE and LILE/HFSE ratios and LILE and LREE enrichment, are strongly indicative of both mantle and crustal contributions. Results of the FC-AFC calculations suggest that interaction with crustal component took probably place at mantle depths, in the case of the group A andesites, through mantle metasomatism by subduction-related fluid/melts of crustal derivation. Partial melting of this enriched mantle source produced the most primitive group A melts that later evolved by simple fractional crystallization processes.

Group F andesites were instead produced by AFC processes taking place during stalling and fractionation of mantle-derived melts in the crust and concurrent assimilation of wall rocks similar to the lower crustal Serre metapelites.

Group VZ dacites and silica-poor ST rocks likely resulted from hybridization, at variable extent, of basaltic mantle magma with pelitic metasediment. Finally, a purely crustal origin by partial melting of a metapelitic source is envisaged for the most acidic dykes, namely the ST silica-rich rhyodacites. Geochemical within-group variations are in this case best modelled in terms of variable entrainment of restite components in the produced melts.

Aknowledgements

This paper benefited by a thorough review of Cristina Perinelli (Rome) and an anonymous reviewer. The Chief Editor Antonio Gianfagna is thanked for his patience in managing the manuscript. Marcello Serracino (IGAG, Rome) is thanked for the help during the EMP analyses.

References

Acquafredda P., Lorenzoni S., Minzoni N. and Zanettin Lorenzoni E. (1987) - The Palaeozoic sequence in the Stilo-Bivongi area (Central Calabria). *Memorie Scienze Geologiche Università Padova*, 39, 117-127.

Acquafredda P., Fornelli A., Paglionico A. and Piccarreta G. (2006) - Petrological evidence for crustal thickening and extension in the Serre granulite terrane (Calabria, southern Italy). *Geological Magazine*, 143, 145-163.

Altherr R. and Siebel W. (2002) - I-type plutonism in a continental back-arc setting: Miocene granitoids and monzonites from the central Aegean Sea, Greece. *Contributions to Mineralogy and Petrology*, 143, 397-415.

Altherr P., Holl A., Hegner E., Langer C. and Kreuzer H. (2000) - High-potassium, calcalkaline Itype plutonism in the European Variscides: Northern Vosges (France) and northern Schwarzwald (Germany). *Lithos*, 50, 51-73.

Alvarez W. (1976) - A former continuation of the Alps. *Geological Society of America Bulletin*, 87, 891-896.

Amodio Morelli L., Bonardi G., Colonna V., Dietrich D., Giunta G., Ippolito F., Liguori V., Lorenzoni S., Paglionico A., Perrone V., Piccarreta G., Russo M., Scandone P., Zanettin-Lorenzoni E. and Zuppetta A. (1976) - L'arco calabro-peloritano nell'orogene appenninico-maghrebide. *Memorie della Società Geologica Italiana*, 17, 1-60.

Angì G., Cirrincione R., Fazio E., Fiannacca P., Ortolano G. and Pezzino A. (2010) - Metamorphic evolution of preserved Hercynian upper crust in the Alpine Calabria-Peloritani Orogen (southern Italy): structural and petrological constraints from the Serre Massif metapelites. *Lithos*, 115, 237-262.

Arculus R.J. (1994) - Aspects of magma genesis in arcs. *Lithos*, 33, 189-208.

Arculus R.J. (2003) - Use and abuse of the terms calcalkaline and calcalkalic. *Journal of Petrology*, 44, 929-935.

Arthaud F. and Matte P. (1977) - Late Palaeozoic strike slip faulting in southern Europe and northern Africa: results of a right lateral shear zone between the Appalachians and the Urals. *Geological Society of American Bullettin*, 88, 1305-1320.

Atzori P. and Traversa G . (1986) - Post-granitic permo-triassic dyke magmatism in eastern Sardinia (Sarrabus pp, Barbagia, Mandrolisai, Goceano, Baronie and Gallura). *Periodico di Mineralogia 55*, 203-231.

Atzori P., Pezzino A. and Rottura A. (1977) - La massa granitica di Cittanova (Calabria Meridionale): relazioni con le rocce granitoidi del massiccio delle Serre e con le metamorfiti di Canolo, San Nicodemo e Molochio (nota preliminare). *Bollettino della Società Geologica Italiana*, 96, 387-391.

Atzori P., Lo Giudice A., Ferla P., Paglionico A., Piccarreta G. and Rottura A. (1981) - Hercynian and pre-Hercynian magmatism in the Calabria-Peloritani Arc (Southern Italy). *Rendiconti della Società Italiana di Mineralogia e Petrologia*, 38, 147-154.

Atzori P., Cirrincione R., Del Moro A. and Mazzoleni P. (2000) - Petrogenesis of late Hercynian calcalkaline dykes of mid-eastern Sardinia: petrological and geochemical data constraining hybridization process. *European Journal of Mineralogy*, 12, 1261-1282.

Avanzinelli R., Lustrino M., Mattei M., Melluso L. and Conticelli S. (2009) - Potassic and ultrapotassic magmatism in the circum-Tyrrhenian region:

significance of carbonated pelitic vs. pelitic sediment recycling at destructive plate margins. *Lithos*, 113, 213-227.

Bonin B. (1989) - Permian volcano-sedimentary events in Corsica: a geological record of a waning Variscan orogeny and its transition to divergent plate boundary processes. *Rendiconti della Società Geologica Italiana*, 42, 139-141.

Bonin B. (2004) - Do coeval mafic and felsic magmas in post-collisional to within-plate regimes necessarily imply two contrasting, mantle and crustal, sources? A review. *Lithos*, 78, 1-24.

Bonin B., Azzouni-Sekkal A., Bussy F. and Ferrag S. (1998) - Alkali-calcic and alkaline post-orogenic (PO) granite magmatism: petrologic constraints and geodynamic settings. *Lithos*, 45, 45-70.

Borsi S. and Dubois R. (1968) - Données géochronologiques sur l'histoire hercynienne et alpine de la Calabre centrale. *Comptes Rendus de l'Académie des Sciences de Paris*, 266, 72-75.

Borsi S., Merlin H.O., Lorenzoni S., Paglionico A. and Lorenzoni-Zanettin E. (1976) - Stilo Unit and "Dioritic-Kinzingitic" Unit in Le Serre (Calabria, Italy). Geological, petrological, geochronological characters. *Bollettino della Società Geologica Italiana*, 95, 219-244.

Bouillin J.P., Durand Delga M. and Olivier Ph. (1986) - Betic-Rifian and Tyrrhenian Arcs: distinctive features, genesis and development stages. In: Wezel F (Eds), The Origin of Arcs. Elsevier, Amsterdam, 281-304.

Caggianelli A., Liotta D., Prosser G. and Ranalli G. (2007) - Pressure-temperature evolution of the late Hercynian Calabria continental crust: compatibility with post-collisional extensional tectonics. *Terra Nova*, 19, 502-514.

Cameron B.I., Walker J.A., Carr M.J., Patino L.C., Matias O. and Feigenson M.D. (2003) - Flux versus decompression melting at stratovolcanoes in southeastern Guatemala. *Journal of Volcanology and Geothermal Research*, 119, 21-50.

Cannic S., Lapierre H., Moni P., Briqueu L. and Basile C. (2002) - Late orogenic evolution of the Variscan lithosphere: Nd isotopic constraints from the western Alps. *Schweizer Mineralogische und Petrographische Mitteilungen*, 82, 77-99.

Carminati E., Lustrino M., Cuffaro M. and Doglioni C. (2010) - Tectonics, magmatism and geodynamics of Italy. What we know and what we imagine. In: The Geology of Italy: tectonics and life along plate margins. M. Beltrando, A. Peccerillo, M. Mattei, S. Conticelli, C. Doglioni (Eds), *Journal of the Virtual Explorer*, 36, doi10.3809/2010.00226.

Cassinis G., Cortesogno L., Gaggero L., Perotti C.R. and Buzzi L. (2008) - Permian to Triassic geodynamic and magmatic evolution of the Brescian Prealps (eastern Lombardy, Italy). *Bollettino della Società Geologica Italiana*, 127, 501-518.

Cirrincione R., Grasso M., Torelli L., Atzori P. and Mazzoleni P. (1995) - The porphyritic clasts of the Tortonian conglomerates of north-central Sicily: paleogeographic and paleotectonic implications. *Bollettino della Società Geologica Italiana*, 114, 131-145.

Colonna V., Lorenzoni S. and Zanettin Lorenzoni E. (1973) - Sull'esistenza di due complessi metamorfici lungo il bordo sud-orientale del massiccio granitico delle Serre (Calabria). *Bollettino della Società Geologica Italiana*, 92, 841-860.

Conticelli S., Laurenzi M.A., Giordano G., Mattei M., Avanzinelli R., Melluso L., Tommasini S., Boari E. (2010) - Leucite-bearing (kamafugitic/leucititic) and -free (lamproitic) ultrapotassic rocks and associated shoshonites from Italy: constraints on petrogenesis and geodynamics. In: The Geology of Italy: tectonics and life along plate margins. M. Beltrando, A. Peccerillo, M. Mattei, S. Conticelli, C. Doglioni (Eds), *Journal of the Virtual Explore*r, 36, 20ISSN 1441-8142.

Cortesogno L., Cassinis G., Dallagiovanna G., Gaggero L., Oggiano G., Ronchi A., Seno S. and Vanossi M. (1998) - The post-Variscan volcanism in the Late Carboniferous-Permian sequences of Ligurian Alps, Southern Alps and Sardinia. *Lithos*, 45, 305-328.

Cortesogno L., Gaggero L., Ronchi A. and Yanev S. (2004a) - Late orogenic magmatism and sedimentation within Late Carboniferous to Early Permian basins in the Balkan terrane (Bulgaria): geodynamic implications. *International Journal of Earth Sciences*, 93, 500-520.

Cortesogno L., Gaggero L. and Yanev S. (2004b) - Anorogenic volcanism in the Triassic sequences at the boundary of the Moesian plate. *Geodinamica Acta*, 17, 55-69.

Critelli S. and Le Pera E. (1998) - Post-Oligocene sediment-dispersal systems and unroofing history of the Calabrian microplate, Italy. *International Geology Review*, 40, 609-637.

D'Amico C., Rottura A., Maccarrone E. and Puglisi G. (1982) - Peraluminous granitic suite of Calabria-Peloritani arc (Southern Italy). *Rendiconti della Società Italiana di Mineralogia e Petrologia*, 38, 35-52.

Dal Piaz G.V. and Martin S. (1998) - Evoluzione litosferica e magmatismo nel dominio austro-sudalpino dall'orogenesi varisica al rifting mesozoico. *Bollettino della Società Geologica Italiana*, 127, 501-518.

Davies J.H. and Stevenson D.J. (1992) - Physical model of source region of subduction zone volcanics. *Journal of Geophysical Research*, 97, 2037-2070.

Del Moro A., Maccarrone E., Pardini G. and Rottura A. (1982) - Studio radiometrico Rb/Sr di granitoidi peraluminosi dell'Arco Calabro Peloritano. *Rendiconti della Società Italiana di Mineralogia e Petrologia*, 38, 1015-1026.

Del Moro A., Fornelli A. and Piccarreta G. (2000) - Disequilibrium melting in granulite-facies metasedimentary rocks of the Northern Serre (Calabria-Southern Italy). *Mineralogy and Petrology*, 70, 89-104.

De Paolo D.J. (1981) - Trace elements and isotopic effects of combined wallrock assimilation and fractional crystallization. *Earth and Planetary Science Letters*, 53, 189-202.

Dewey J.F., Helman M.L., Turco E., Hutton D.H.W. and Knott S.D. (1989) - Kinematics of the western Mediterranean. In: Alpine Tectonics. (eds): M.P. Coward, D. Dietrich, R.G. Park, *Geological Society of London, Special Publication*, 45, 265-283.

Doglioni C. (1992) - Una interpretazione della tettonica globale. *Le Scienze*, 270, 32-42.

Ersoy Y. and Helvacı C. (2010) - FC-AFC-FCA and mixing modeler: A Microsofts Excel and spreadsheet program for modeling geochemical differentiation of magma by crystal fractionation, crustal assimilation and mixing. *Computers and Geosciences*, 36, 383-390.

Fiannacca P., Williams I.S., Cirrincione R. and Pezzino A. (2008) - Crustal Contributions to Late Hercynian Peraluminous Magmatism in the Southern Calabria Peloritani Orogen, Southern Italy: Petrogenetic Inferences and the Gondwana Connection. *Journal of Petrology*, 49, 1897-1514.

Finger F. and Steyrer H.P. (1990) - I-type granitoids as indicator of late Paleozoic convergent ocean-continent margin along the southern flank of the central European Variscan orogen. *Geology*, 18, 1207-1210.

Franzini M., Leoni L. and Saitta M. (1975) - Revisione di una metodologia analitica per fluorescenza-X, basata sulla correzione completa degli effetti di matrice. *Rendiconti della Società Italiana di Mineralogia e Petrologia*, 31, 365-378.

Gerlach D.C., Frey F.A., Moreno-Roa H., Lopez-Escobar L. (1988) - Recent volcanism in the Puyehue-Cordon Caulle region, Southern Andes, Chile (40.5°S): petrogenesis of evolved lavas. *Journal of Petrology*, 29, 333-382.

Gill J.B. (1981) - Orogenic Andesites and Plate Tectonics. Berlin.

Gorton M.P. and Schandl E.S. (2000) - From continent to island arcs: a geochemical index of tectonic setting for arc related and within plate felsic to intermediate volcanic rocks. *The Canadian Mineralogist, 38*, 1065-1073.

Graessner T., Schenck V., Brocker M. and Mezger K. (2000) - Geochronological constraints on timing of granitoid magmatism, metamorphism and post-metamorphic cooling in the Hercynian crustal cross-section of Calabria. *Journal of Metamorphic Geology*, 18, 409-421.

Grove T.L. and Kinzler R.J. (1986) - Petrogenesis of andesites. *The Annual Review of Earth and Planetary Sciences*, 14, 417-454.

Gueguen E., Doglioni C. and Fernandez M. (1998) - On the post-25 Ma geodynamic evolution of the western Mediterranean. *Tectonophysics*, 298, 259-269.

Guerrera F., Martın-Algarra A. and Perrone V. (1993) - Late Oligocene-Miocene syn-late-orogenic successions in Western and Central Mediterranean Chains from the Betic Cordillera to the Southern Apennines. *Terra Nova*, 5, 525-544.

Haccard D., Lorentz C. and Grandjacquet C. (1972) - Essal sur l'èvolution tectogénétic de la liason Alpes-Apennines (de la Ligurie à la Calabre). *Memorie della Società Geologica Italiana*, 11, 309-341.

Hawkesworth C.J., Gallagher K., Hergt J.M. and McDermott F. (1993) - Mantle slab contributions in arc magmas. *The Annual Review of Earth and Planetary Sciences*, 21, 175-204.

Hawkesworth C.J., Turner S., Gallagher K., Hunter A., Bradshaw T. and Rogers N. (1995) - Calcalkaline magmatism, lithosphere thinning and extension in the Basin and Range. *Journal of Geophysical Research*, 100, 10271-10286.

Janousek V., Bowes D.R., Rogers G., Farrow C.M. and Jelinek E. (2000) - Modelling diverse processes in the petrogenesis of a Composite Batholith: the Central Bohemian Pluton, Central European Hercynides. *Journal of Petrology*, 41, 511-543.

Johnson R.W., Mackenzie D.E. and Smith I.E.M. (1978) - Delayed partial melting of subduction-modified mantle in Papua New Guinea. *Tectonophysics*, 46, 197-216.

Innocenti C., Briqueu L. and Cabanis B. (1994) - Sr-Nd isotope and trace element geochemistry of late Variscan volcanism in the Pyrenees: Magmatism in post-orogenic extension? *Tectonophysics*, 238, 161-181.

Irvine T.N. and Baragar W.R.A. (1971) - A guide to the chemical classification of the common volcanic rocks. *Canadian Journal of Earth Sciences*, 8, 523-548.

Knott S.D. (1987) - The liguride complex of southern Italy - Cretaceous to Paleogene accretionary wedge. *Tectonophysics*, 142, 217-226.

Lago M., Arranz E., Pocovi A., Galè C. and Gil-Imaz A. (2004) - Permian magmatism and basin dynamics in the southern Pyrenees: a record of the transition from late Variscan transtension to early Alpine extension. In: Permo-Carboniferous magmatism and rifting in Europe. (eds): M. Wilson, E.R. Neumann, M.J. Timmerman, M. Heeremans and B. Larsen, *Geological Society of London, Special Publication,* 223*,* London, 439-464.

Leake B.E., Woolley A.R., Arp C.E.S., Birch W.D., Gilbert M.C., Grice J.D., Hawthorne F.C., Kato A., Kisch H. J., Krivovichev V.G., Linthout K., Laird J., Mandarino J., Maresch W.V., Nichel E.H. and Rock N.M.S. (1997) - Nomenclature of amphibole. Report of the Subcommission on Amphiboles of the International Mineralogical Association Commission on New Minerals and Mineral Names. *European Journal of Mineralogy*, 9, 623-651.

Ledru P., Courrioux G., Dallain C., Lardeaux J.M., Montel J.M., Vanderhague O. and Vitel G. (2001) - The Velay dome (French Massif Central): melt generation and granite emplacement during orogenic evolution. *Tectonophysics*, 342, 207-237.

Lorenz V. and Nicholls I.A. (1984) - Plate and intraplate processes of Hercynian Europe during the late Paleozoic. *Tectonophysics*, 107, 25-56.

Lustrino M. (2000) - Phanerozoic geodynamic evolution of the circum-Italian realm. *International Geology Review,* 42, 724-757.

Lustrino M., Morra V., Fedele L. and Franciosi L. (2009) - Beginning of the Apennine subduction system in central western Mediterranean: constraints from Cenozoic "orogenic" magmatic activity of Sardinia (Italy). *Tectonics*, 28, TC5016, doi:10.1029/2008TC002419.

Lustrino M., Duggen S. and Rosenberg C. (2011) - The Central-Western Mediterranean: anomalous igneous activity in an anomalous collisional tectonic setting. *Earth-Science Reviews*, 104, 1-40.

McDonough W.F. and Sun S.-S (1995) - The composition of the Earth. *Chemical Geology*, 120, 223-253.

Miller C.F., Stoddard E.F., Bradfish L.J. and Dollase W. A. (1981) - Composition of plutonic muscovite; genetic implications. *The Canadian Mineralogist*, 19, 25-34.

Morimoto N. (1988) - Nomenclature of pyroxenes. *Mineralogical Magazine*, 52, 535-550.

Nakamura N. (1974) - Determination of REE, Ba, Fe, Mg, Na and K in carbonaceous and ordinary chondrites. *Geochimica et Cosmochimica Acta*, 38, 757-775.

Ogniben L. (1969) - Schema introduttivo alla geologia del confine calabro-lucano. *Memorie della Società Geologica Italiana*, 8, 453-763.

Orejana D., Villaseca C., Billstrom K. and Paterson B.A. (2008) - Petrogenesis of Permian alkaline lamprophyres and diabases from the Spanish Central System and their geodynamic context within western Europe. *Contributions to Mineralogy and Petrology*, 156, 477-500.

Ortolano G., Cirrincione R. and Pezzino A. (2005) - P-T evolution of Alpine metamorphism in the southern Aspromonte Massif (Calabria - Italy). *Schweizer Mineralogische und Petrographische Mitteilungen*, 85, 31-56.

Pearce J.A. (1982) - Trace elements characteristics of lavas from destructive plate boundaries. In: Thorpe R.S. (Eds), Andesites, John Wiley and Sons.

Pearce J.A. (1983) - The role of sub-continental litosphere in magma genesis at destructive plate margins. In: Continental basalts and mantle xenoliths. (eds): C.J. Hawkesworth, M.J. Norry, Nantwich: Shiva, 230-249.

Pearce J.A. (1996) - Sources and settings of granitic rocks. *Episodes*, 19, 120-125.

Pearce J.A. and Peate D.W. (1995) - Tectonic

implications of the composition of volcanic arc magma. *Annual Review of Earth and Planetary Sciences*, 23, 251-285.

Pearce J.A., Harris N.B.W and Tindle A.G. (1984) - Trace element discrimination diagrams for the tectonic interpretation of granitic rocks. *Journal of Petrology*, 25, 956-983.

Peccerillo A. and Martinotti G. (2006) - The Western mediterranean lamproitic magmatism: origin and geodynamic significance. *Terra Nova*, 18, 109-117.

Peccerillo A. and Taylor S.R. (1976) - Geochemistry of Eocene calcalkalinevolcanic rocks from the Kastamonu area, northern Turkey. *Contributions to Mineralogy and Petrology*, 58,63-81.

Perini G., Cebria J.M., Ruiz J.L. and Doblas M. (2004) - Carboniferous-Permian mafic magmatism of volcanic and subvolcanicrocks in the Variscan belt of Spain and France: implications for mantle sources. In: Permo-Carboniferous Rifting and Magmatism in Europe. (eds): M. Wilson, E.R. Neumann, G.R. Davies, M.J. Timmerman, M. Heeremans, B.T. Larsen, *Geological Society of London, Special Publication*, 223, 415-438.

Rapp R.P. and Watson E.B. (1995) - Dehydration melting of metabasalt at 8-32 kbar: Implications for continental growth and crust-mantle recycling. *Journal of Petrology*, 36, 891-931.

Rosenbaum G., Lister G.S. and Duboz C. (2002) - Relative motions of Africa, Iberia and Europe during Alpine orogeny. *Tectonophysics*, 359, 117-129.

Rosenberg C.L. (2004) - Shear zones and magma ascent: a model based on a review of the Tertiary magmatism in the Alps. *Tectonics*, 23, Doi:10.1029/2003TC001526.

Rottura A., Bargossi G.M., Caironi V., Del Moro A., Maccarrone E., Macera P., Paglionico A., Petrini R., Piccarreta G. and Poli G. (1990) - Petrogenesis of contrasting Hercynian granitoids from the Calabrian Arc, southern Italy. *Lithos,* 24, 97-119.

Rottura A., Del Moro A., Pinarelli L., Petrini R., Peccerillo A., Caggianelli A., Bargossi G. and Piccarreta G. (1991) - Relationships between intermediate and acidic rocks in orogenic granitoid suite: petrological, gerochemical and isotopic (Sr, Nd, Pb) data from Capo Vaticano (Southern Calabria, Italy). *Chemical Geology*, 92, 153-176.

Rottura A., Caggianelli A., Campana R. and Del Moro A. (1993) - Petrogenesis of Hercynian peraluminous granites from the Calabrian Arc, Italy. *European Journal of Mineralogy*, 5, 737-754.

Rottura A., Bargossi G.M., Caggianelli A., Del Moro A., Visonà D. and Tranne C.A. (1998) - Origin and significance of the Permian high-K calc-alcaline magmatism in the central-eastern Southern Alps, Italy. *Lithos*, 45, 329-348.

Rudnick L.R. and Gao S. (2003) - Composition of the continental crust. In: Treatise on Geochemistry. (eds): R.L. Rudnick, *Elsevier*, 3, 1-64.

Schenk V. (1980) - U-Pb and Rb-Sr radiometric dates and their correlation with metamorphic events in the granulitic-facies basement of the Serra, Southern Calabria (Italy). *Contributions to Mineralogy and Petrology*, 73, 23-38.

Schenk V. (1984) - Petrology of felsic granulites, metapelites, metabasics, ultramafics, and metacarbonates from southern Calabria (Italy): prograde metamorphism, uplift and cooling of a former lower crust. *Journal of Petrology*, 25, 255-298.

Schenk V. (1990) - The exposed crustal cross section of southern Calabria, Italy: structure and evolution of a segment of Hercynian crust. In: Salisbury M.H., Fountain D.M. (Eds), Exposed cross section of the continental crust. Kluwer Dordrecht, The Netherlands, 21-42.

Shimizu N. and Arculus R.J. (1975) - Rare earth concentrations in a suite of basanitoids and alkaline olivine basalts from Grenada, lesser Antilles. *Contributions to Mineralogy and Petrology*, 50, 231-240.

Stampfli G.M. and Borel G.D. (2002) - A plate tectonic model for the Paleozoic and Mesozoic constrained by dynamic plate boundaries and restored synthetic oceanic isochrons. *Earth and Planetary Science Letters*, 196, 17-33.

Stampfli G.M., Borel G.D., Marchant R. and Mosar J. (2002) - Western Alps geological constraints on Western Tethyan reconstruction. *Journal of the Virtual Explorer*, 7, 75-104.

Stille P. and Buletti M. (1987) - Nd-Sr isotopic characteristic of the Lugano volcanic rocks and constraints on the continental crust formation in the South Alpine domain (N Italy-Switzerland). *Contribution to Mineralogy and Petrology*, 96, 140-150.

Tatsumi Y. (1989) - Migration of fluid phases and genesis of basalt magmas in subduction zone. *Journal of Geophysical Research*, 94, 4697-4707.

Tortorici L. (1982) - Lineamenti geologico-strutturali dell'Arco Calabro Peloritano. *Rendiconti della Società Italiana di Mineralogia e Petrografia*, 4, 927-940.

Tortorici L., Catalano S. and Monaco C. (2009) - Ophiolite-bearing mélanges in southern Italy. *Geological Journal*, 44, 153-166.

Traversa G., Ronca S., Del Moro A., Pasquali C., Buraglini N. and Barabino G. (2003) - Late to post-Hercynian dyke activity in the Sardinia-Corsica Domain: A transition from orogenic calcalkaline to anorogenic alkaline magmatism. *Bollettino della Società Geologica Italiana, Special Volume*, 2, 131-152.

Ulrych J., Pesek J., Stepankova-Svobodovay A.J., Bosak P., Lloyd F.E., Von Seckendorff V., Lang M. and Novak J.K. (2006) - Permo-Carboniferous volcanism in late Variscan continental basins of the Bohemian Massif (Czech Republic): geochemical characteristic. *Chemie der Erde*, 66, 37-56.

Von Blanckenburg F., Kagami H., Deutsch A. and Oberli F. (1998) - The origin of Alpine plutons along the Periadriatic Lineament. *Schweizerische Mineralogische und Petrographische Mitteilungen*, 78, 55-66.

Winchester J.A. and Floyd P.A. (1977) - Geochemical discrimination of different magma series and their differentiation products using immobile elements. *Chemical Geology*, 20, 325-343.

Wilson M., Tankut A. and Gulec N. (1997) - Tertiary volcanism of the Galatia Province, north-west Central Anatolia, Turkey. *Lithos*, 42, 105-121.

Ziegler P. A. (1993) - Late Palaeozoic-Early Mesozoic Plate re-organization: evolution and demise of the Variscan fold belt. In: Pre-Mesozoic in the Alps. (eds): J.F. von Raumer and F. Neubauer, *Springer*, Berlin Heidelberg New York, 171-201.

Submitted, August 2011 - Accepted, November 2011